Physikalisch-Technische Bundesanstalt

PTB

WGDM-7: Preliminary Comparison on Nanometrology According to the rules of CCL key comparisons

NANO 2

STEP HEIGHT STANDARDS

FINAL REPORT

Braunschweig, 26. Aug. 2003 / L. Koenders

Appendix

1   INTRODUCTION

The discussion group for Nanometrology (WGDM7 DG) decided at their meeting at the BIPM in June 98 that preliminary comparisons should be carried out using five different types of artefacts. One set of artefacts chosen were step height standards. These comparisons are likely to be proposed at a later date as key comparisons. The rules for the organisation of key comparisons should therefore be followed[1]. The pilot laboratory for this ***preliminary comparison*** on step height standards was the Physikalisch-Technische Bundesanstalt (PTB).

2   STANDARDS

2.1   GENERAL REQUIREMENTS

At the WGDM7 DG meeting, the general opinion was that the step height standards should cover the range from the nanometre to the several micro metre range. The standards should meet the requirements of different measuring methods using, for example, stylus instruments (ST), interference microscopes (IM) and other optical instruments as well as scanning probe microscopes (SPM). The participants should have the liberty to choose the method preferred by them.

2.2   DESCRIPTION OF THE STANDARDS

A set of step height standards manufactured by the Fraunhofer Institute of Microstructure Stuttgart, for the PTB was used for the comparison. They are available with step heights between 7 nm and 800 nm. The standards consist of a 5 mm x 5 mm silicon chip, glued on a sample holder 12 mm in diameter. The surface of these standards is made conductive and opaque by a Chromium layer, approximately 100 nm in thickness. There are three lines on the standards. The widths are 5 µm, 30 µm and 100 µm (fig. 1). For the use of scanning probe microscopes, interference microscopes as well as stylus instruments it has been decided to use the right line with a width of 30 µm as indicated in fig. 2.

In addition to the circulated set each participating institute got a complete set of standards from the PTB for their own use. The idea was that the participating laboratories should measure their own standards at the same time under the same conditions as the standards used for the WGDM7 comparison.

2.3   COMMENT

After first start in May 2000 the Nano2 comparison was stopped due to problems with an unknown contamination of the used standards. Therefore another type of standard – as described above - was used to minimise the time delay and to restart as fast as possible. The standards were initially characterised at PTB by interference microscope, stylus instrument and a commercial SPM, because the metrology SPM was on move from PTB Berlin to Braunschweig.

---

[1] T. J. Quinn, Guidelines for key comparisons carried out by Consultative Committees, March 1, 1999, BIPM, Paris
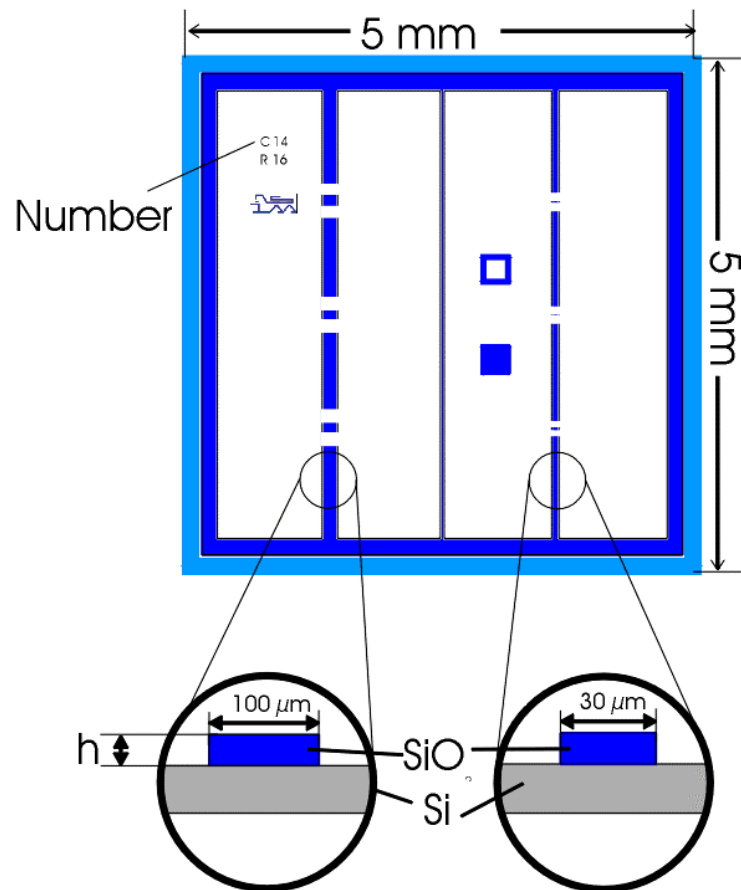
Fig. 1. Layout of the step height standard. The substrate is Silicon, the lines are SiO$_2$, and the whole sample is covered by a Chromium layer (not shown). There are three lines with widths of 5 µm, 30 µm and 100 µm. The samples are glued on a thin steel disc with a diameter of 12 mm.

Fig. 2. The line used for the comparison has a width of 30 µm and is located on the right side. The field R1 which should be used for the measurements is shown on the right drawing.

3   PARTICIPANTS AND TIME SCHEDULE

3.1   ORGANISATION

Following the rules set up by the BIPM [2] a small group of participating laboratories has drafted this technical protocol. The group was composed of the pilot laboratory and two participating members (Ted Vorburger, NIST, USA; Joergen Garnaes, DFM, Denmark; Ludger Koenders, PTB, Germany). By their declared intention to participate in this 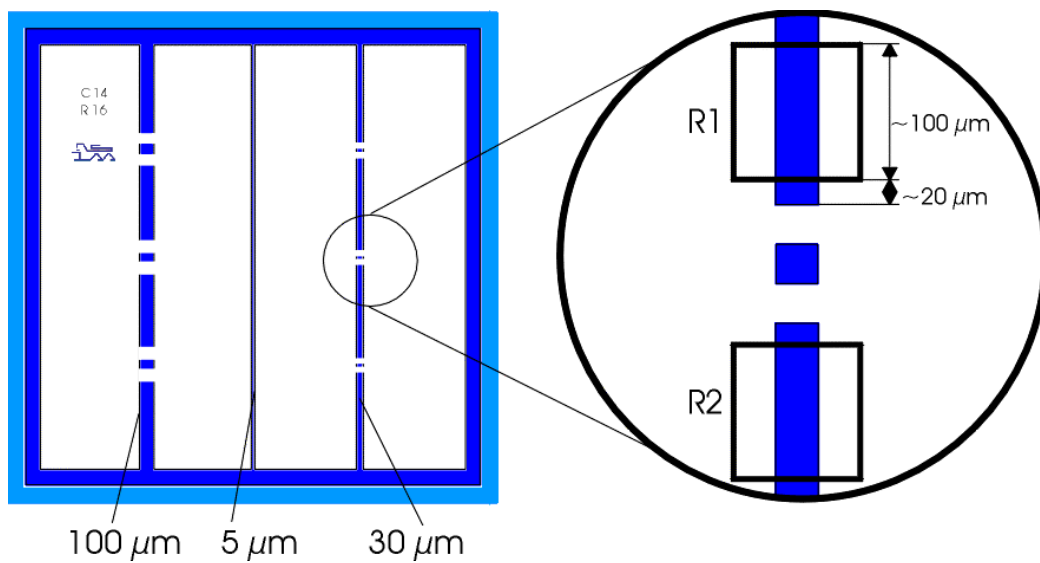preliminary comparison, the participants accepted the general instructions and the technical protocols written down in the *NANO2 - Technical Protocol* document which was sent to them and committed themselves to follow the procedures.

3.2   REQUIREMENTS FOR PARTICIPATION

According to the WGDM recommendation No 2 (document CCDM/WGDM/97-50b), the participating laboratories should offer this measurement as a calibration service (now or in future) and be willing to participate in a regional comparison in order to provide a link between the interregional and the regional comparisons.

3.3   PARTICIPANTS IN THE CIRCULATION

The participants of this preliminary comparison are listed in table 1.

Table 1. Participating laboratories

Laboratory	*Responsible*	*Address*	*Phone: Fax, e-mail*
CEM	E. Prieto	Centro Español de Metrologia Del Alfar, 2 28760 Tres Cantos / Madrid Spain	Phone: +34 91 8074 716 Fax: +34 91 8074 807 e-mail: eprieto@mfom.es
CMS	Gwo-Sheng Peng	Center for Measurement Standards (CMS/ITRI) Bldg. 16 321 Kuang Fu Rd, Sec. 2 Hsinchu, Taiwan 300	Phone: +886 3 574 3773 Fax: +886 3 572 6445 e-mail: Gwo-Sheng.Peng@itri.org.tw
METAS	F. Meli	Swiss Federal Office of Metrology and Accreditation Lindenweg 50 CH-3003 Bern-Wabern Switzerland	Phone: +41 31 323 3346 Fax: +41 31 323 3210 e-mail: felix.meli@metas.admin.ch
DFM	J. Garnaes	Danish Institute of Fundamental Metrology Building 307 Anker Engelunds Vej 1 DK-2800 Lyngby Denmark	Phone: +45 45 25 5884 Fax: +45 45 93 1137 e-mail: jg@dfm.dtu.dk

---

[2] see http://www.bipm.fr/enus/8_Key_Comparisons/key_comparisons.html

GUM	B. Smereczynska	Central Office of Measures (Glowny Urzad Miar GUM) Length and Angle Division Surface Texture Measurements Laboratory 2 Elektoralna St. 00-950 Warsaw, POLAND	Phone: +48 22 620 54 38 Fax: +48 22 620 83 78 e-mail: length@gum.gov.pl
IMGC	G. B. Picotto	CNR Istituto di Metrologia "G. Colonnetti" Strada delle Cacce, 73 I-10135 Torino Italy	Phone: +39 011 39 469/473 Fax: +39 011 39 77 459 e-mail: g.picotto@imgc.cnr.it
KRISS	Byong Chon Park	Korea Research Institute of Standards and Science Length Group 1 Toryong-dong Yusong Taejon 305 – 340 Republic of Korea	Phone: +82 42 868 5105 Fax: +82 42 868 5608 e-mail: bcpark@kriss.re.kr
NIM	Gao Sitian	National Institute of Metrology Length Division No 18, Bei San Huan Dong Lu BEIJING 100013 China	Phone: +86 10 6421 8703 Fax: +86 10 6421 8627 e-mail: gaost@nim.ac.cn
NIST	T. Vorburger	National Institute of Standards and Technology NIST Room A117, Metrology Building Gaithersburg, MD 20899-0001 USA	Phone: +1 301 975 3493 Fax: +1 301 869 0822 e-mail: tvtv@nist.gov
NMi-VSL	R. Bergmans	NMi - Van Swinden Laboratorium Schoemakerstraat 97 2600 AR DELFT The Netherlands	Phone: +31 15 269 1641 Fax: +31 15 261 2971 e-mail: Rbergmans@NMi.nl
NPL	K. Jackson	National Physical Laboratories Centre for Basic, Thermal and Length Metrology Building 3, Queens Road Teddington, Middlesex, TW11 0LW United Kingdom	Phone: + 44 20 8943 6218 Fax: + 44 20 86140420 e-mail: keith.jackson@npl.co.uk
NMIJ	T. Kurosawa	Lengths and Dimensions Division National Metrology Institute of Japan Advanced Semiconductor Res. Center National Institut of Advanced Industrial Sciences and Technology (AIST) 1-1-1, Umezono TSUKUBA IBARAKI 305-8563 Japan	Phone: +81 298 61 4041 Fax: +81 298 61 4042 e-mail: tomizo.kurosawa@aist.go.jp

VNIIM	A. N. Korolev	D.I.Mendeleyev Institute for Metrology 19, Moskovsky pr. St. Petersburg, 198005 Russia	Phone: 007 812 251-8638 Fax: 007 812 113-0114 e-mail: ank@rol.ru or A.N.Korolev@vniim.ru
Pilot laboratory			
PTB	L. Koenders	Physikalisch-Technische Bundesanstalt 5.12 Mikro- und Nanotopographie Bundesallee 100 D- 38116 Braunschweig Germany	Phone: +49 531 592 5120 Fax: +49 531 592 5105 e-mail: Ludger.Koenders@ptb.de

3.4 TIME SCHEDULE

After the stop of the NANO2 comparison due to the failure of the first set of standards it could already be restarted in September 2000. It was carried out in a mixed form, circulation and star type. The period of time available to each laboratory was one month for calibration including transportation to the next participant.

As the sample were contaminated during the circulation some additional cleaning procedures and therefore a transport to the pilot laboratory was necessary. Additionally from September 2001 on an ATA CARNET was used to facilitate the transportation. Nevertheless, due to problems at customs, especially for transport to and from the VNIIM, the comparison needed more time than planned and proposed in the time schedule. The transport to VNIIM and back to the pilot lab took some weeks each direction. A more detailed description is given in Appendix B.

Table 2: Time schedule (short)

Lab.	Country	Original schedule	Confirmation of reception	Comment	Results received
PTB	Germany	1.9.2000	-	IM and ST only*)	1.9.2000
IMGC	Italy	1.10.2000	22.9.2000	cantilever on SH800	2.4.2002
NMi-VSL	Netherlands	1.11.2000	15.11.2000		9.1.2001
CEM	Spain	1.12.2000	12.12.2000		7.3.2001
DFM	Denmark	15.1.2001	No conform.		4.2.2002
PTB	*2nd circle*			*by passed to METAS*	
METAS	Switzerland	1.3.2001	22.2.2001		8.4.2001
NIM	China	1.7.2001	4.4.2001		3.4.2002
CMS	Taiwan	1.5.2001	18.5.2001		27.11.2001
NMIJ	Japan	1.6.2001	8.6.2001	cantilever on SH300	28.9.2001

KRISS	Korea	1.8.2001	20.7.2001		6.5.2002
PTB	*3rd circle*	*1.9.2001*	*5.9.2001*	*IM and ST only*)*	
NPL	United Kingdom	1.10.2001	11.10.2001	tip crash on SH300	20.2.2002
PTB			*16.11.2001*	*by passed to GUM*	
GUM	Poland	1.11.2001	7.12.2001		25.2.2002
PTB			*14.1.2002*	*by passed to VNIIM*	
VNIIM	Russia	1.12.2002	18.2.2002		29.4.2002
PTB			*12.4.2002*	*by passed to NIST*	
NIST	USA	1.4.2001	18.4.2002	Cleaning of SH20 at NIST	
PTB			*5.6.2002*	*Cleaning SH007 and back to NIST*	
NIST	USA		14.6.2002	SH007 at NIST	5.9.2002
PTB		*15.1.2002*	*9.7.2002*	*IM, ST, SPM*)*	*3.9.2002*

*) At the failure of the first set of standards, the metrology SPM of the PTB was moving from Berlin to Braunschweig and was not available for measurements. Due to some time delays in Sept. 2001, it was not possible to measure before July 2002.

4   MEASURAND

4.1   EVALUATION OF THE STEP HEIGHT

The measurand to be determined was the step height as defined in fig. 3. For the comparison the measurements should be performed **on the 20, 70 and 800 nm standard within the area denoted as R1 (see fig 2). The standards with 7 and 300 nm step height were optional.** The step height h is defined in analogy to ISO 5436, taking into consideration the restriction of some SPM that should be used in the comparison.
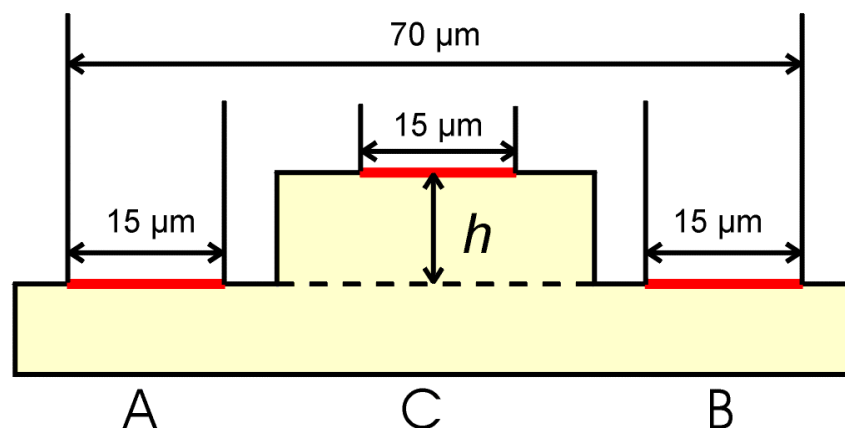

Fig. 3. Definition of step height h used in the comparison

A continuous straight mean line should be drawn over the marked areas of the measured profile to represent the lower level of the surface and another representing the upper level, both lines extending symmetrically about the centre of the line (fig. 3). The height h is defined as the perpendicular distance of the mean of the portion C to the line through the mean of portion A and the mean of portion B.

The measurand to be used in this comparison was the average height obtained from different measurements within the reference area R1. A significant number of measurements, not less than five, at evenly distributed positions should be taken.

4.2 REPORT

The participants could state more than one measurement result if they have applied different techniques. For each method, a detailed estimation of the measurement uncertainty according to the ISO *Guide to the Expression of Uncertainty in Measurement (GUM)* should be given. The amount of time available for measurements by one participant is independent of the number of methods applied. If possible, a comparison with the laboratory's own set of standards (see above) should be made in parallel. The measured step height h has to be stated for the reference temperature at 20°C.

5 MEASUREMENT METHODS

The participants are free to choose their own method of measurement, like stylus instruments (ST), interference microscopes (IM) and other optical instruments as well as scanning probe microscopes (SPM). By this a comparison between the different methods is possible, although the conditions could be critical for some of them. Each participant could supply results from different methods. CEM, NMIJ, NIST, PTB, and VNIIM have supplied results for two up to three methods while all others used one method. Table 3 gives an overview. The full description of the measurement methods and instruments by the participants can be found in appendix A.

Table 3. Methods of measurements

No	Institute	Method	Instruments	Traceability
1	CEM 1	IM	Interferential microscope MicroXAM-Ex from Phase Shift Technology	Calibrated using several steps/grooves with certified values (NIST, NMi-VSL)
2	CEM 2	ST	Stylus profiler Dektak^3 ST from Veeco.	Calibrated using several steps/grooves with certified values (NIST, NMi-VSL)
3	CMS	SPM	Commercial AFM with capacitive position sensors (DI metrology head). Image analysis with SPIP software.	Step height reference standards is from by VLSI Standards Incorporated (STS2-1800S) (traceable to NIST)

4	DFM	SPM	Commercial AFM with capacitive position sensors (DI metrology head). A special calibration software was used (SPIP).	Step height standard H800 from Nanosensors calibrated at PTB
5	GUM	IM	Linnik's type micro-interferometer (type MII-4)	Green light (λ = 536,6 nm)
6	IMGC	ST	Stylus profilometer (Talystep 1, Taylor Hobson- RTH)	Displacement piezo-actuators with capacitve transducers (DPT-10 from Queensgate) which have been calibrated using a heterodyne interferometer
7	KRISS	ST	Stylus instrument (Nanostep 2, Taylor Hobson Ltd., UK),	Gauge block calibrated by interferometer at KRISS
8	METAS	SPM	OFMET AFM profiler with interferometric long range linear displacement stage. AFM with DI metrology head.	Laser traceable to OFMET standards
9	NMIJ1	IM	Interferometric microscope with a Mirau-type interferometric objective	Laser interferometer
10	NMIJ2	SPM	AFM with three-axis laser interferometer	Laser traceable to NMIJ standards
11	NMi-VSL	IM	Zeiss Interphako interference microscope with phase modulator and digital readout of the phase adjustments.	546,23 nm line of a mercury discharge lamp
12	NIM	SPM	AFM VERITEKT 3 with integrated laser interferometer	Laser traceable to NIM standards
13	NIST 1	SPM	NIST C-AFM with heterodyne laser interferometer, closed loop control of the lateral sample positioning system.	633 nm wavelength of the I_2-stabilized He-Ne laser
14	NIST 2	ST	Talystep stylus instrument	Interferometrically measured step
15	NPL	SPM	NPL Metrological Atomic Force Microscope (MAFM) with integrated laser interferometers in 3 axis	Laser traceable to NPL standards
16	PTB 1	IM	Zeiss interference microscope with CCD-system	Thallium lamp (λ=535 nm).
17	PTB 2	SPM	Veritekt B with integrated laser interferometers in x,y, and z.	Lasers traceable to PTB standards
18	PTB 3	ST	Nanostep (Taylor-Hobson) stylus instrument	Step gauges calibrated by interference microscope

Final Report

19	VNIIM 1	LHI	Laser heterodyne interferometer with a single-frequency He-Ne laser and acousto-optical modulators	Laser traceable to VNIIM standards
20	VNIIM 2	µI	Michelson micro interferometer illuminated by the light of Ar or He-Ne lasers	Lasers traceable to VNIIM standards

6 STABILITY OF THE STANDARDS

Each participant was asked to inspect the standards after reception (see Nano2 Technical Report - Appendix B) and to send a report to the pilot laboratory. Due to some problems with SPMs and their cantilevers and due to a larger amount of dust in the reference areas it was unavoidable to clean some of standards during the comparison. The overall quality of the step height standards decreased continuously during the comparison, mainly due to dust contamination. However, the reference area R1 on the standards remained almost unchanged. Only the SH70 step height was damaged within the R1 area so that a small part of the reference area R1 could not be measured. However, this did not influence the measurement results, with one exception (see PTB(IM)).

The stability of the standards were monitored by different calibrations performed by the pilot laboratory during the comparison. Stylus and interference microscope calibrations were made in Sept. 2000, Sept. 2001 and May 2002 (see table 4). The results show that - with the exception of the first measurement by interference microscope of the SH070 at PTB - no significant change in the step height could be observed.

Table 4. Stability of the standards as measured by interference microscope (standard uncertainty u)

IM	SH007		SH020		SH070		SH300		SH800	
	h /nm	u /nm	h /nm	u /nm	h /nm	u /nm	h /nm	u /nm	h /nm	u /nm
01.09.00	6,50	1,00	19,80	1,00	65,40	1,70	292,00	1,80	781,00	3,30
19.09.01	6,40	0,90	20,00	1,00	67,70	1,15	292,70	1,60	779,20	3,40
30.06.02	6,30	0,90	20,80	1,00	67,50	1,20	292,40	1,80	780,80	3,40
Mean/nm	6,40		20,20		66,87		292,37		780,33	
Stdev/nm	0,10		0,53		1,27		0,35		0,99	

7 MEASUREMENT RESULTS

In the following the results received from all the participants are presented. Besides the measured values for the step height h, the combined standard uncertainty u_c, the degree of freedom ν_{eff} and the expanded uncertainty U(k=2) is given. The other values En, h_{ir}, and U_{ir} are explained below. The receipt date (see table 2) is used as the measurement date; in the case of DFM it was set to the 15.1.2002.

7.1   RESULTS ON STEP HEIGHT STANDARD SH007 (OPTIONAL)

Table 5.1. Step height standard SH007 (Optional)

SH007	Institute	Meas.	h / nm	u_c / nm	$\nu_{eff}(h)$	k	$U(k=2)$/ nm	En **)	$|h_{ir}|$ / nm	U_{ir} / nm
ST	CEM(ST)	12.12.00	6,34	0,79	38	2	1,58	0,05	0,08	1,56
	IMGC(ST)	22.09.00	6,7	0,4	14	2	0,80	0,33	0,28	0,76
	KRISS(ST)	20.07.01	6,39	0,41	17,1	2	0,82	0,04	0,03	0,79
	NIST(ST)	05.09.02	6,31	0,42	18,8	2	0,84	0,13	0,11	0,81
	PTB(ST)	26.06.00	7,0	1,8	59	2	3,60	0,16	0,58	3,59
IM	CEM(IM)	12.12.00	6,24	0,61	37	2	1,22	0,15	0,18	1,20
	GUM(IM)	07.12.01								
	NMIJ(IM)	08.06.01	5,94	0,14	24,2	2	0,28	1,2*)		
	NMi-VSL(IM)	15.11.00	6,01	0,25	52,6	2	0,50	0,75	0,41	0,44
	PTB(IM)	26.06.00	6,5	1,0	28	2	2,00	0,04	0,08	1,99
	VNIIM(LHI)	18.02.02								
	VNIIM(LMM)	18.02.02								
SPM	CMS(SPM)	18.05.01	7,5	0,9	50	2	1,80	0,59	1,08	1,78
	DFM(SPM)	15.01.01								
	METAS(SPM)	22.02.01	5,99	0,47	195	2	0,94	0,45	0,43	0,91
	NMIJ(SPM)	08.06.01	7,019	0,225	4,5	2	0,45	1,43*)		
	NIM(SPM)	04.04.01	6,17	1,8	40	2	3,60	0,07	0,25	3,59
	NIST(SPM)	18.04.02	6,74	0,39	14,3	2	0,78	0,39	0,32	0,74
	NPL(SPM)	11.10.01	6,67	0,23	5,0	2	0,46	0,48	0,25	0,40
	PTB(SPM)	09.07.02	6,4	0,80	79	2	1,60	0,01	0,02	1,58

*) 1st calculation results in En =1,43 and En =1,20 for NMIJ(SPM) and NMIJ(IM), respectively (see text).
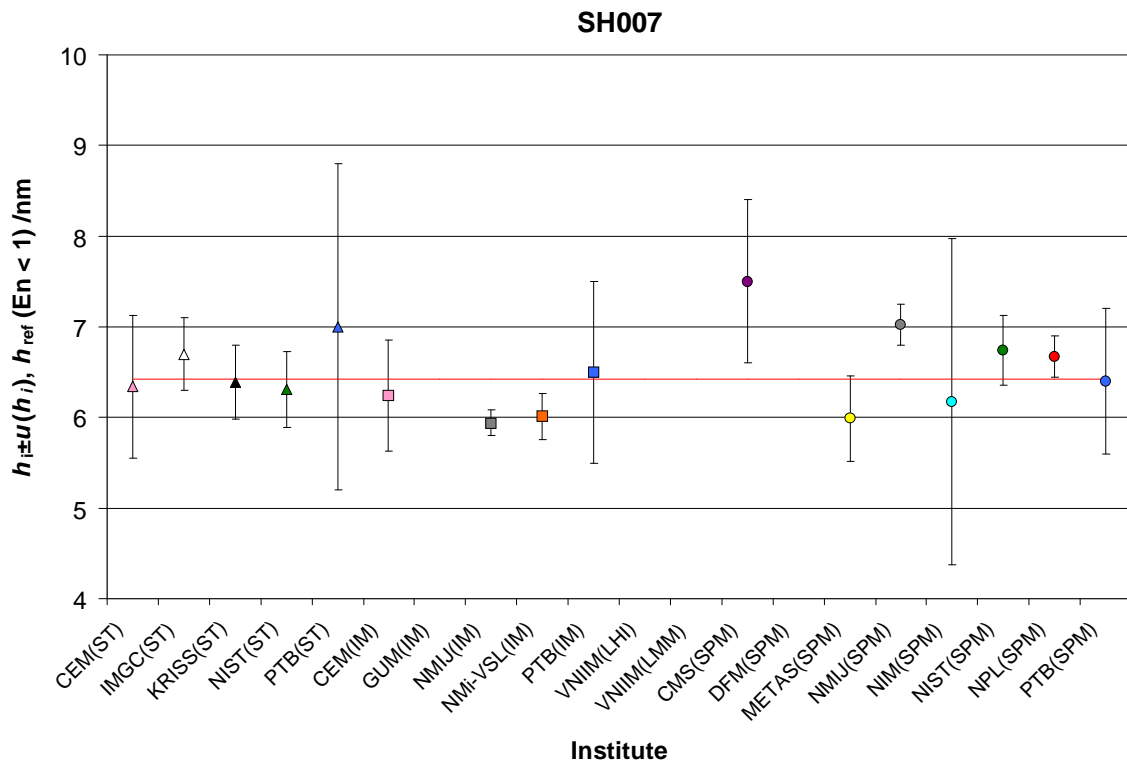**) 2nd calculation of En without the NMIJ(SPM) and NMIJ(IM) values.

Fig. 4.1. Measured step heights h_i of the institute and reference value h_{ref} (red line) calculated from the En<1 values only.

7.2 RESULTS ON STEP HEIGHT STANDARD SH020

Table 5.2. Step height standard SH020

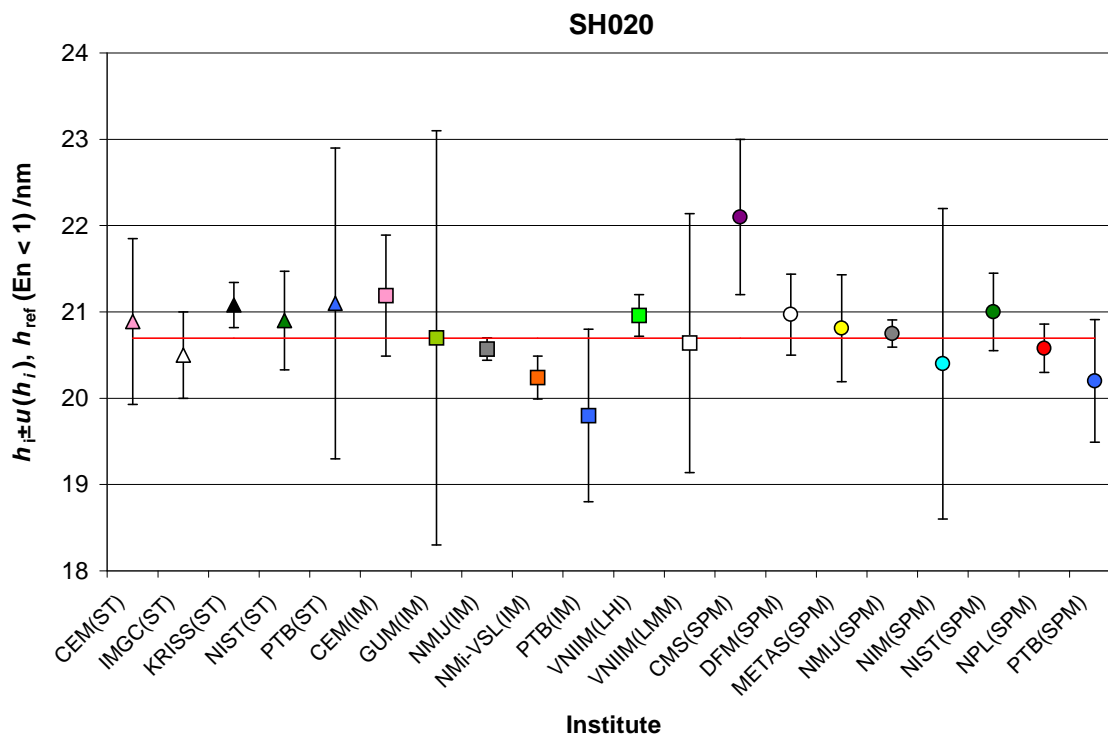| SH020	Institute	Meas.	h / nm	u_c / nm	$v_{eff}(h)$	k	$U(k{=}2)$ / nm	En *)	$|h_{ir}|$ / nm	U_{ir} / nm
ST	CEM(ST)	12.12.00	20,89	0,96	45	2	1,92	0,10	0,19	1,91
	IMGC(ST)	22.09.00	20,5	0,5	32	2	1,00	0,20	0,20	0,99
	KRISS(ST)	20.07.01	21,08	0,26	8,9	2	0,52	0,71	0,38	0,50
	NIST(ST)	05.09.02	20,90	0,57	36,9	2	1,14	0,18	0,20	1,13
	PTB(ST)	26.06.00	21,1	1,8	61	2	3,60	0,11	0,40	3,60
IM	CEM(IM)	12.12.00	21,19	0,70	59	2	1,40	0,35	0,49	1,39
	GUM(IM)	07.12.01	20,7	2,4	9	2	4,80	0,00	0,00	4,80
	NMIJ(IM)	08.06.01	20,57	0,13	21,7	2	0,26	0,43	0,13	0,22
	NMi-VSL(IM)	15.11.00	20,24	0,25	73,0	2	0,50	0,88	0,46	0,48
	PTB(IM)	26.06.00	19,8	1,0	29	2	2,00	0,45	0,90	1,99
	VNIIM(LHI)	18.02.02	20,96	0,24	166	2	0,48	0,52	0,26	0,46
	VNIIM(LMM)	18.02.02	20,64	1,5	17	2	3,00	0,02	0,06	3,00
SPM	CMS(SPM)	18.05.01	22,1	0,9	56	2	1,80	0,78	1,40	1,79
	DFM(SPM)	15.01.01	20,97	0,47	100	2	0,94	0,29	0,27	0,93
	METAS(SPM)	22.02.01	20,81	0,62	46	2	1,24	0,09	0,11	1,23
	NMIJ(SPM)	08.06.01	20,750	0,156	94,6	2	0,31	0,15	0,05	0,28
	NIM(SPM)	04.04.01	20,4	1,8	39	2	3,60	0,08	0,30	3,60
	NIST(SPM)	18.04.02	21,00	0,45	19,5	2	0,90	0,33	0,30	0,89
	NPL(SPM)	11.10.01	20,58	0,28	10,1	2	0,56	0,20	0,12	0,54
	PTB(SPM)	09.07.02	20,2	0,71	83	2	1,42	0,35	0,50	1,41

*) En after 1st calculation

Fig. 4.2. Measured step heights h_i of the institute and reference value h_{ref} (red line) calculated from the En<1 values only.

Final Report

7.3 RESULTS ON STEP HEIGHT STANDARD SH070

Table 5.3. Step height standard SH070

SH070	Institute	Meas.	h / nm	u_c / nm	$\nu_{eff}(h)$	k	$U(k=2)$ / nm	En **)	$|h_{ir}|$ / nm	U_{ir} / nm
ST	CEM(ST)	12.12.00	68,00	1,06	67	2	2,12	0,22	0,47	2,10
	IMGC(ST)	22.09.00	67,3	0,7	60	2	1,40	0,16	0,23	1,38
	KRISS(ST)	20.07.01	67,57	0,72	26,5	2	1,44	0,02	0,04	1,42
	NIST(ST)	05.09.02	67,10	0,49	28,4	2	0,98	0,43	0,43	0,94
	PTB(ST)	26.06.00	68,1	1,8	59	2	3,60	0,16	0,57	3,59
IM	CEM(IM)	12.12.00	68,87	0,80	66	2	1,60	0,82	1,34	1,58
	GUM(IM)	07.12.01	68,1	2,50	10	2	5,00	0,11	0,57	4,99
	NMIJ(IM)	08.06.01	67,29	0,21	13,7	2	0,42	0,50	0,24	0,33
	NMi-VSL(IM)	15.11.00	68,0	0,5	34	2	1,00	0,45	0,47	0,97
	PTB(IM)	26.06.00	65,4	1,7	9	2	3,40	0,63	2,13	3,39
	VNIIM(LHI)	18.02.02	68,55	0,25	233	2	0,50	1,45*)		
	VNIIM(LMM)	18.02.02	68,45	1,25	67	2	2,50	0,36	0,92	2,49
SPM	CMS(SPM)	18.05.01	67,7	1,1	85	2	2,20	0,07	0,17	2,18
	DFM(SPM)	15.01.01	68,17	0,62	100	2	1,24	0,50	0,64	1,21
	METAS(SPM)	22.02.01	68,20	0,47	171	2	0,94	0,68	0,67	0,90
	NMIJ(SPM)	08.06.01	67,061	0,510	9,8	2	1,02	0,45	0,47	0,99
	NIM(SPM)	04.04.01	67,7	2,0	71	2	4,00	0,04	0,17	3,99
	NIST(SPM)	18.04.02	67,56	0,43	22,6	2	0,86	0,03	0,03	0,82
	NPL(SPM)	11.10.01	66,74	1,26	8,3	2	2,52	0,31	0,79	2,51
	PTB(SPM)	09.07.02	67,9	0,75	86	2	1,50	0,24	0,37	1,48

*) 1st calculation results in En =1,45 for VNIIM(LHI)

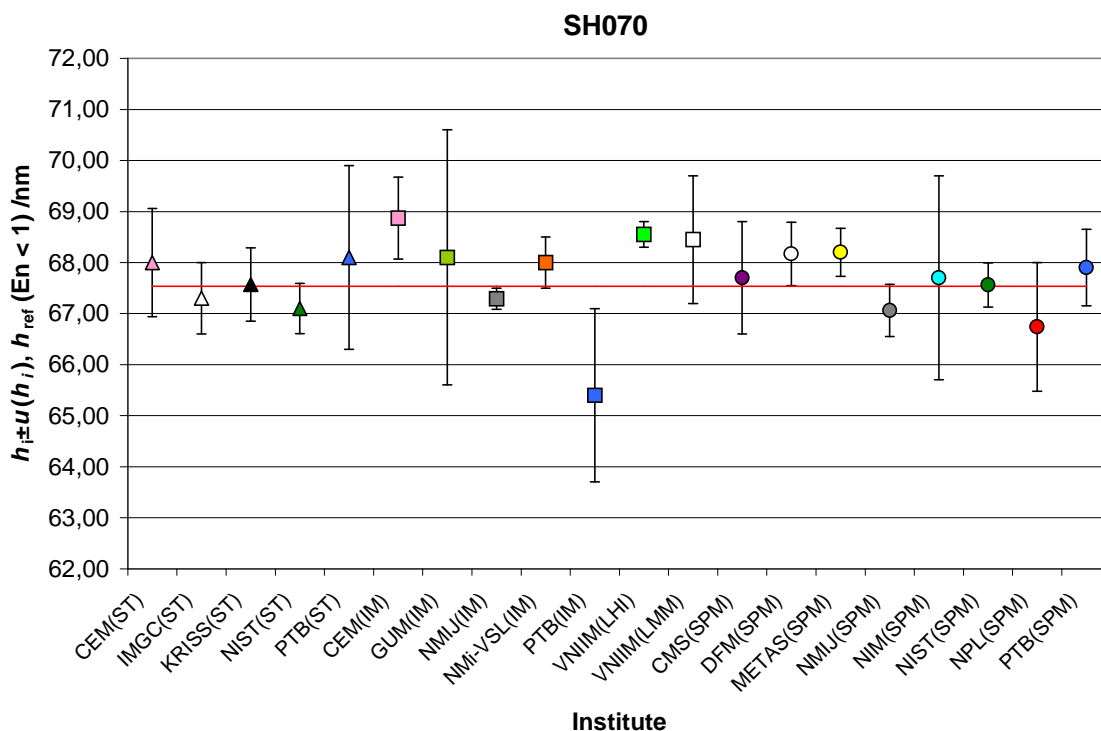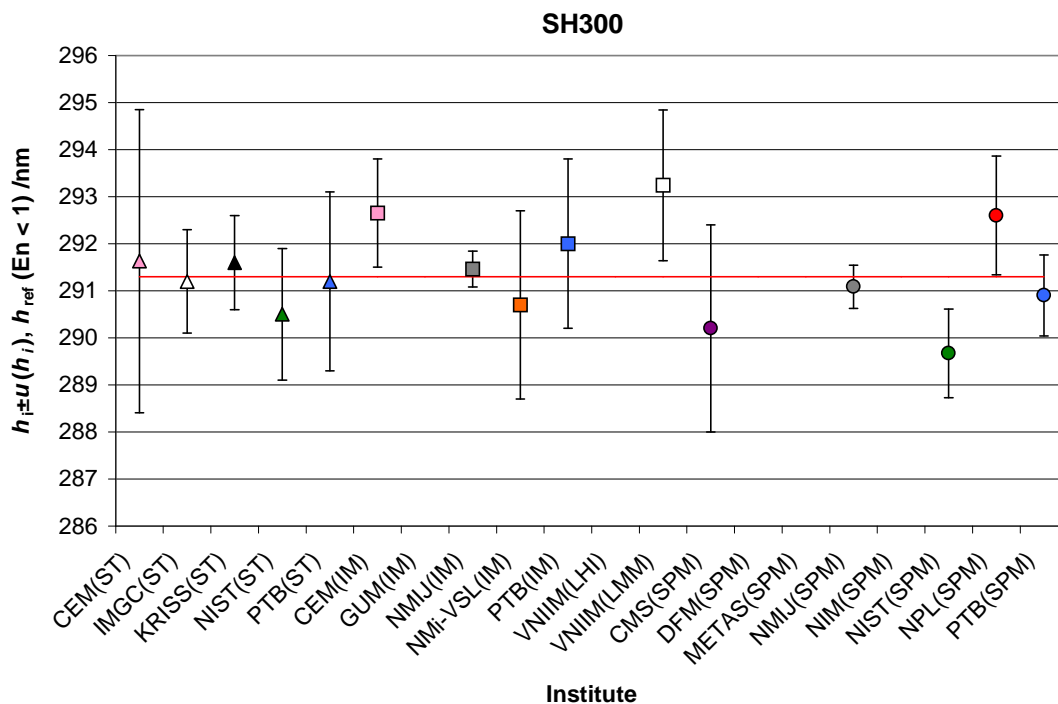**) 2nd calculation without the VNIIM (LHI) value

Fig. 4.3. Measured step heights h_i of the institute and reference value h_{ref} (red line) calculated from the En<1 values only.

7.4 RESULTS ON STEP HEIGHT STANDARD SH300 (OPTIONAL)

Table 5.4. Step height standard SH300 (Optional)

SH300	Institute	Meas.	h / nm	u_c / nm	$v_{eff}(h)$	k	$U(k{=}2)$/ nm	En **)	$|h_{ir}|$ / nm	U_{ir} / nm
ST	CEM(ST)	12.12.00	291,63	3,22	34	2	6,44	0,05	0,33	6,42
	IMGC(ST)	22.09.00	291,2	1,1	67	2	2,20	0,04	0,10	2,15
	KRISS(ST)	20.07.01	291,6	1,0	201,6	2	2,00	0,15	0,30	1,95
	NIST(ST)	05.09.02	290,5	1,4	5,6	2	2,80	0,28	0,80	2,76
	PTB(ST)	26.06.00	291,2	1,9	60	2	3,80	0,03	0,10	3,77
IM	CEM(IM)	12.12.00	292,65	1,15	74	2	2,30	0,58	1,35	2,25
	GUM(IM)	07.12.01								
	NMIJ(IM)	08.06.01	291,46	0,38	14,5	2	0,76	0,18	0,16	0,61
	NMi-VSL(IM)	15.11.00	290,7	2,0	24,2	2	4,00	0,15	0,60	3,97
	PTB(IM)	26.06.00	292	1,8	34	2	3,60	0,19	0,70	3,57
	VNIIM(LHI)	18.02.02								
	VNIIM(LMM)	18.02.02	293,24	1,6	68	2	3,20	0,60	1,94	3,17
SPM	CMS(SPM)	18.05.01	290,2	2,2	49	2	4,40	0,25	1,10	4,38
	DFM(SPM)	15.01.01								
	METAS(SPM)	22.02.01	285,01	0,64	49	2	1,28	*)		
	NMIJ(SPM)	08.06.01	291,084	0,458	17,0	2	0,92	0,21	0,21	0,80
	NIM(SPM)	04.04.01								
	NIST(SPM)	18.04.02	289,67	0,94	316	2	1,88	0,84	1,63	1,82
	NPL(SPM)	11.10.01	292,60	1,26	24,4	2	2,52	0,51	1,30	2,48
	PTB(SPM)	09.07.02	290,9	0,86	40	2	1,72	0,22	0,40	1,66

*) Result from METAS has been withdrawn (see comment METAS SPM, p. 44)
**) En after 1st calculation

Fig. 4.4. Measured step heights h_i of the institute and reference value h_{ref} (red line) calculated from the En<1 values only.

7.5 RESULTS ON STEP HEIGHT STANDARD SH800

Table 5.5. Step height standard SH800

SH800	Institute	Meas.	h / nm	u_c / nm	$v_{eff}(h)$	k	$U(k=2)$ / nm	En ***)	$|h_{ir}|$ / nm	U_{ir} / nm
ST	CEM(ST)	12.12.00	778,22	7,51	23	2	15,02	0,01	0,17	15,01
	IMGC(ST)	22.09.00	778,1	2,1	69	2	4,20	0,07	0,29	4,15
	KRISS(ST)	20.07.01	780,1	2,5	196,8	2	5,00	0,34	1,71	4,96
	NIST(ST)	05.09.02	776,5	2,1	45,4	2	4,20	0,44	1,89	4,15
	PTB(ST)	26.06.00	780,0	2,0	57	2	4,00	0,40	1,61	3,95
IM	CEM(IM)	12.12.00	782,30	2,29	34	2	4,58	0,85	3,91	4,53
	GUM(IM)	07.12.01	773,7	3,6	20	2	7,20	0,65	4,69	7,17
	NMIJ(IM)	08.06.01	776,14	0,80	18,8	2	1,60	1,13**)		
	NMi-VSL(IM)	15.11.00	778,0	5,2	23,6	2	10,40	0,04	0,39	10,38
	PTB(IM)	26.06.00	781	3,3	32	2	6,60	0,39	2,61	6,57
	VNIIM(LHI)	18.02.02	778,60	0,46	251	2	0,92	0,19	0,21	0,66
	VNIIM(LMM)	18.02.02	778,4	2,0	88	2	4,00	0,00	0,01	3,95
SPM	CMS(SPM)	18.05.01	781,7	5,7	40	2	11,40	0,29	3,31	11,38
	DFM(SPM)	15.01.01	782,8	4,4	100	2	8,80	0,50	4,41	8,78
	METAS(SPM)	22.02.01	759,33	0,65	171	2	1,30	*)		
	NMIJ(SPM)	08.06.01	777,46	0,705	8,8	2	1,41	0,60	0,93	1,25
	NIM(SPM)	04.04.01	777,1	2,0	61	2	4,00	0,32	1,29	3,95
	NIST(SPM)	18.04.02	779,8	2,5	378	2	5,00	0,28	1,41	4,96
	NPL(SPM)	11.10.01	777,24	2,61	527	2	5,22	0,22	1,15	5,18
	PTB(SPM)	09.07.02	778,4	1,18	53	2	2,36	0,00	0,01	2,27

*) Result from METAS has been withdrawn (see comment METAS SPM, p. 44)

**) 1st En calculation value gives En =1,13 for NMIJ(IM)

***) 2nd En calculation without the result of NMIJ(IM)
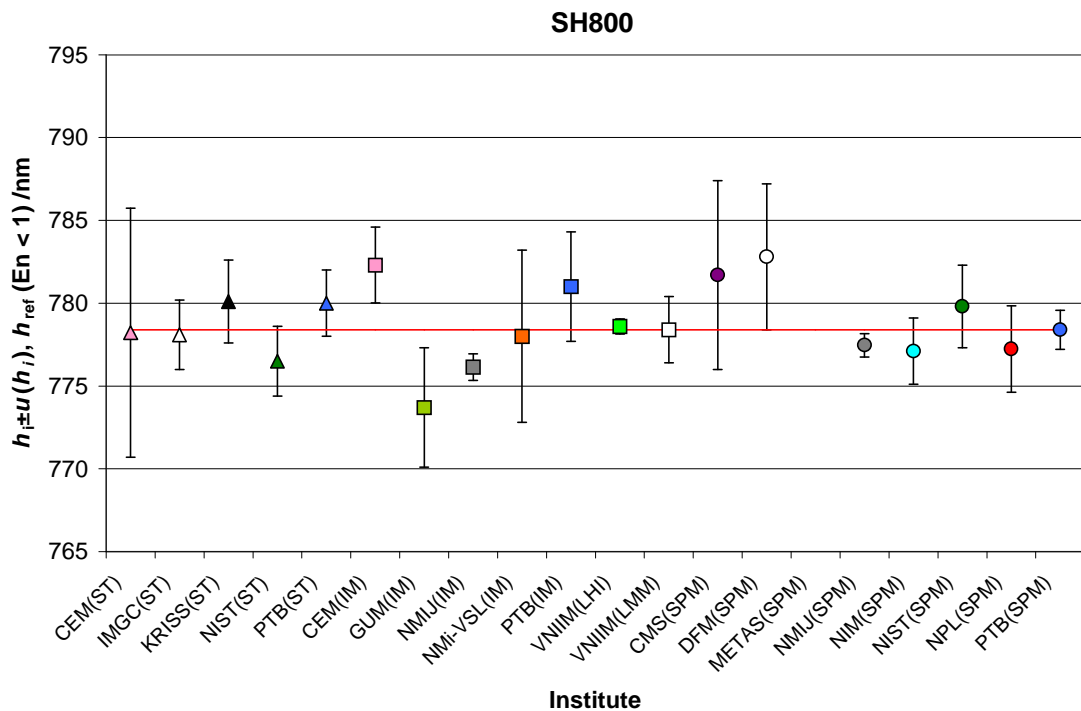
Fig. 4.5. Measured step heights h_i of the institute and reference value h_{ref} (red line) calculated from the En<1 values only.

Final Report

8 UNCERTAINTY BUDGET

The uncertainty of the measurement is to be estimated according to the *Guide to the Expression of Uncertainty in Measurement*. The participating laboratories were encouraged to use all known influence parameters for the method applied by them. The step height h of the standards is expressed as a function of the input quantities X_i

$$h= f(x_i). \tag{1}$$

The combined standard uncertainty $u_c(h)$ is the square sum of the standard uncertainties of the input quantities $u(x_i)$, each weighted by a sensitivity coefficient c_i

$$u_c^2(h) = \sum_i c_i^2 u^2(x_i) \text{ with } \qquad c_i = \frac{\partial h}{\partial x_i}. \tag{2}$$

The uncertainty components should be divided into components associated with the realisation of the object compared, and those associated with the comparison method.

Contributions to the uncertainty budgets depends on the method and the instrument used:
1. calibration
-   vacuum wavelengths of lasers
-   refraction index of the air
-   interferometer alignment
-   uncertainty of calibrated standards used
-   non-linearity of the instrument
-   angular motion of translation stages
-   Abbe offset

2. measurement
-   sample alignment
-   noise of instrument
-   repeatability

3. evaluation
-   roughness of the standard
-   out of plane motion
-   temperature of the standard

9 ANALYSIS

9.1 REFERENCE VALUE AND ITS UNCERTAINTY

The reference value (h_{ref}) for this step height comparison is calculated as the weighted mean of all measurements (h_i). The weights are $u^{-2}(h_i)$. For each step height standard a reference value was calculated. To set up the $|En| \leq 1$ criterion [3], the expanded uncertainty

---

[3] http://www.euromet.org/pages/guides/guide.htm in Guidelines for the organisation of comparisons

U with a coverage factor of k = 2 was used [4]. Measurements with En values larger than one have to be omitted one by one for the calculation of the reference value. By this all values contributing to the reference value have En values smaller than one.

$$\text{Reference value} \qquad h_{ref} = \frac{\sum_{i=1}^{n} u^{-2}(h_i) \cdot h_i}{\sum_{i=1}^{n} u^{-2}(h_i)} \qquad (3)$$

$$\text{Combined standard uncertainty} \qquad u_c(h_{ref}) = \left(\sum_{i=1}^{n} u^{-2}(h_i) \right)^{-\frac{1}{2}} \qquad (4)$$

$$\text{Degree of freedom} \, v_{eff}(h_{ref}) = \frac{u_c^4(h_{ref})}{\sum_{i=1}^{n} \frac{u_i^4(h_{ref})}{v_{eff}(h_i)}} \quad \text{with} \quad u_i(h_{ref}) = |c_i| \cdot u(h_i) = \frac{u^{-1}(h_i)}{\sum_{i=1}^{n} u^{-2}(h_i)} \qquad (5)$$

$$\text{Expanded uncertainty using k=2} \qquad U(h_{ref}, k=2) = 2 \cdot u_c(h_{ref}) \qquad (6)$$

$$\text{En-criteria} \qquad En(h_i) = \left| \frac{h_i - h_{ref}}{\sqrt{U^2(h_i) + U^2(h_{ref})}} \right| \qquad (7)$$

The plus sign in the denominator of (7) is used although there is some correlation between a single measurement result and the reference value. With the plus sign the En values could be slightly too small [5].

For the calculation of the comparison reference value only 4 of the totally 90 [6] measurements had to be omitted. The corresponding En values for each step height standard before the exclusion were[7]:

SH007: 1st calculation gives NMIJ(IM) En = 1,20 and NMIJ(SPM) En = 1,43. In this case the values which were measured at the same institute do not overlap within two times their uncertainty interval! The successive removal procedure as described above would be more or less arbitrary. Therefore both values are omitted for the calculation of the reference value! This problem has to be solved within the institute, first.

SH020: All measurement results fulfil the En criteria.

SH070: The first calculation results in En = 1,45 for VNIIM(LHI).

SH300: Result of METAS(SPM) was withdrawn (see comment METAS SPM p. 44). The other measurement results fulfil the En criteria.

SH800: Result of METAS(SPM) was withdrawn (see comment METAS SPM p. 44). The calculation of En results in En = 1,13 for NMIJ(IM).

---

[4] W. Wöger, Remarks on the E_n –Criterion Used in Measurem. Comp.: PTB-Mitteilungen 109 (1999) 24
[5] see comment 8 in chapter 10, too.
[6] Two measurement results were withdrawn.
[7] These deviations could not be clarified during the discussion finally.

The reference values calculated of the remaining results are listed in table 6 together with their uncertainties and the calculated Birge ratio R_B.

The Birge ratio $\qquad R_B = \dfrac{u_{ext}}{u_{in}}$ $\qquad\qquad\qquad\qquad\qquad\qquad$ (8)

with $\quad u_{ext} = \sqrt{\dfrac{\sum\limits_{i=1}^{n}\left[(h_i - h_{ref})/u_i\right]^2}{(n-1)\sum\limits_{i=1}^{n}u^{-2}(h_i)}}$ $\quad$ and $u_{in} = u_c(h_{ref})$ $\qquad\qquad$ (9)

is calculated to check the statistical consistency of a comparison. It compares the observed spread of results u_{in} with the spread of the estimated uncertainty u_{ext}. A value of R_B close to 1 or less suggest that results are consistent, whereas values much greater than 1 suggest that results are inconsistent. [8]

Table 6. Reference value h_{ref}, $U(h_{ref}, k=2)$, R_B for each standard (En<1), n number of measurements

Standard	h_{ref} / nm	$u(h_{ref})$ / nm	$U(h_{ref},k=2)$ / nm	ν_{eff}	R_B	n
SH007	6,42	0,12	0,23	61	0,77	14
SH020	20,70	0,07	0,15	157	0,84	20
SH070	67,53	0,13	0,26	82	0,85	19
SH300	291,30	0,23	0,45	79	0,78	15
SH800	778,39	0,32	0,64	164	0,82	18

The Birge ratio R_B calculated is in the range of 0,8. This shows that the mean uncertainty is overestimated, but is based on a small number of measurements. This can occur if the uncertainty budget of one institute is overestimated compared to their deviations from the reference values. For example, the NIM values are relative close to the reference value, but their uncertainty budget is large compared to this.

9.2   DEGREE OF EQUIVALENCE

The degree of equivalence (DoE) of each laboratory with respect to the reference value is given by DoE(h_{ir}, U_{ir}) defined as:

$$h_{ir} = h_i - h_{ref} \quad \text{and} \quad U_{ir} = 2*\sqrt{(u_i^2 - u_{ref}^2)}. \qquad (10)$$

Here the corresponding uncertainties u_i and u_{ref} cannot simply be geometrically added, because the values h_i and h_{ref} are correlated [9]. These values are given in the tables above for each standard. A plot of the values of U_{ir} as function of the absolute difference $h_{ir} = h_i - h_{ref}$ for each institute is shown in the following figures.

---

[8] R. Kacker, R. Datla, A. Parr, metrologia 39 (2002) p. 279 - 293
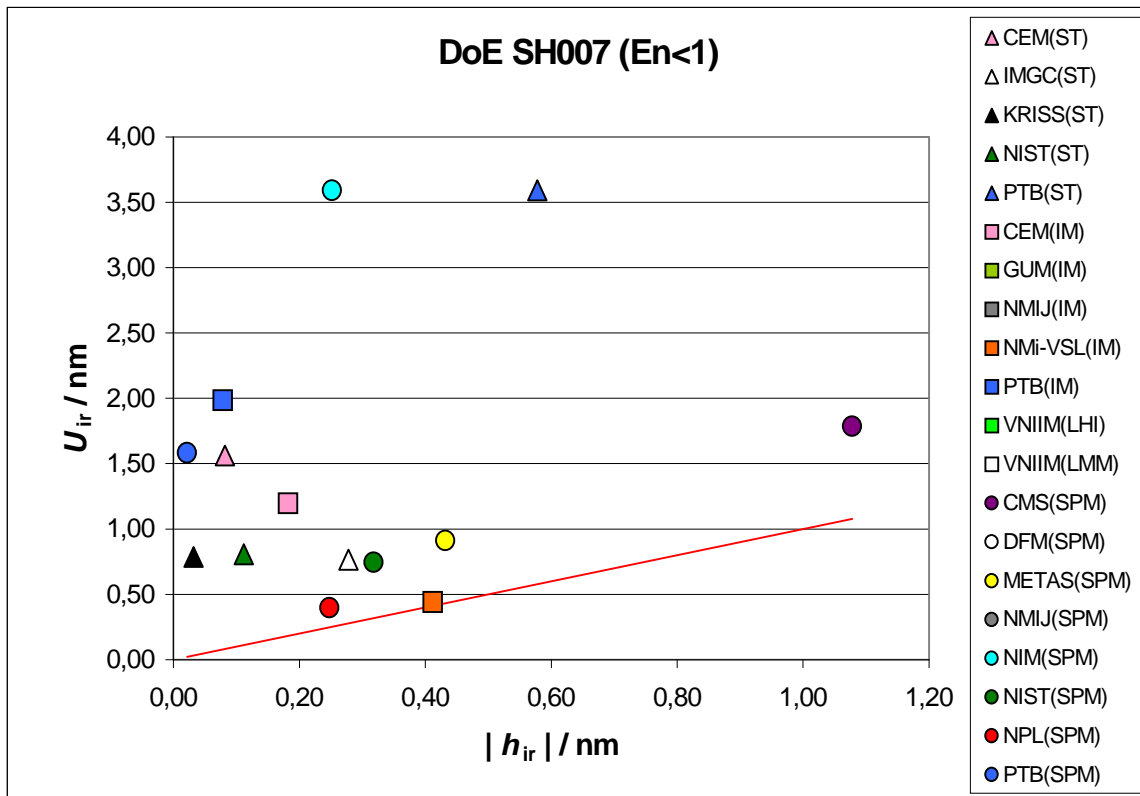[9] R. Thalmann, Metrologia 39 (2002) p. 165 – 177

Fig. 5.1. Degree of equivalence for the SH007. The U_{ir} values are plotted as function of the absolute deviation from the reference value $h_{ir} = h_i - h_{ref}$.
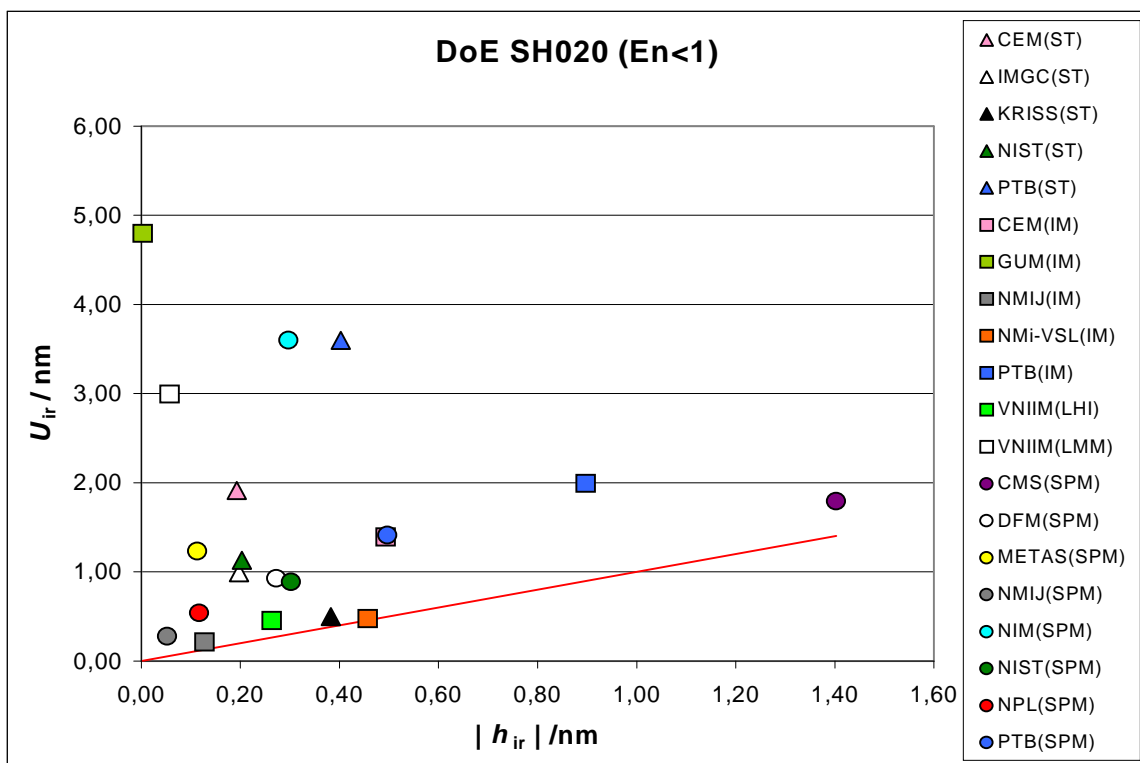

Fig. 5.2. Degree of equivalence for the SH020. The U_{ir} values are plotted as function of the absolute deviation from the reference value $h_{ir} = h_i - h_{ref}$.
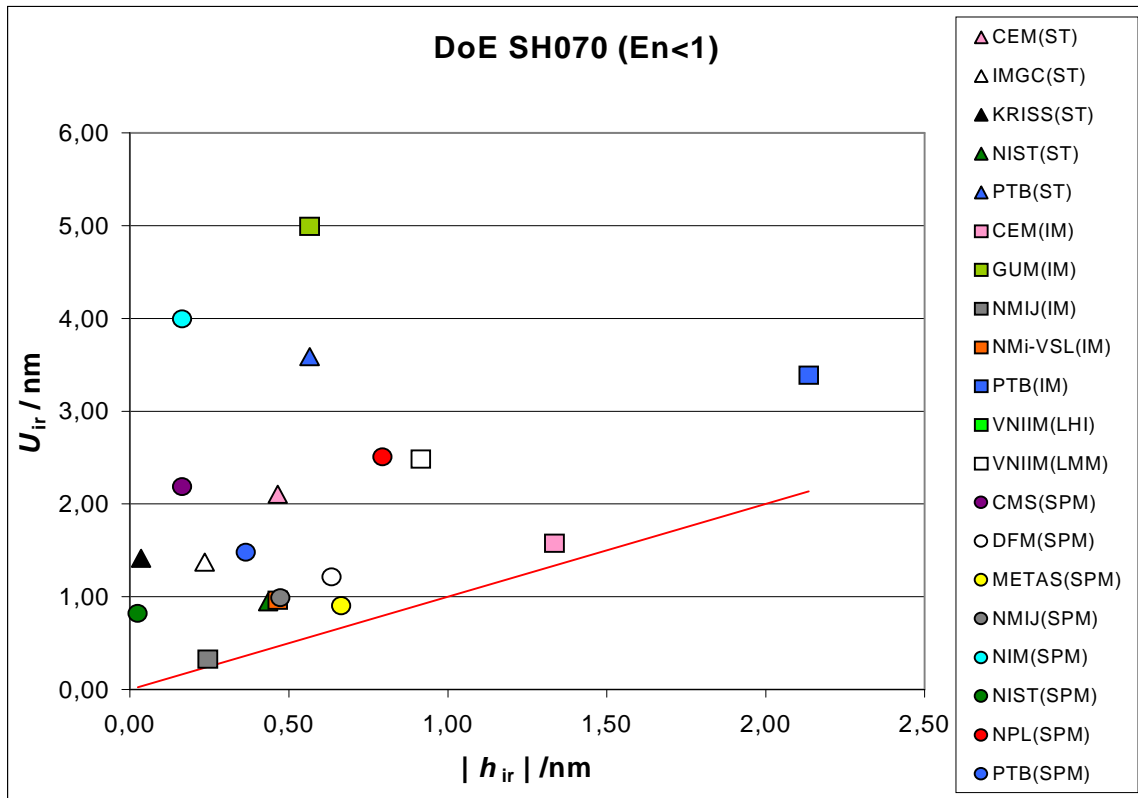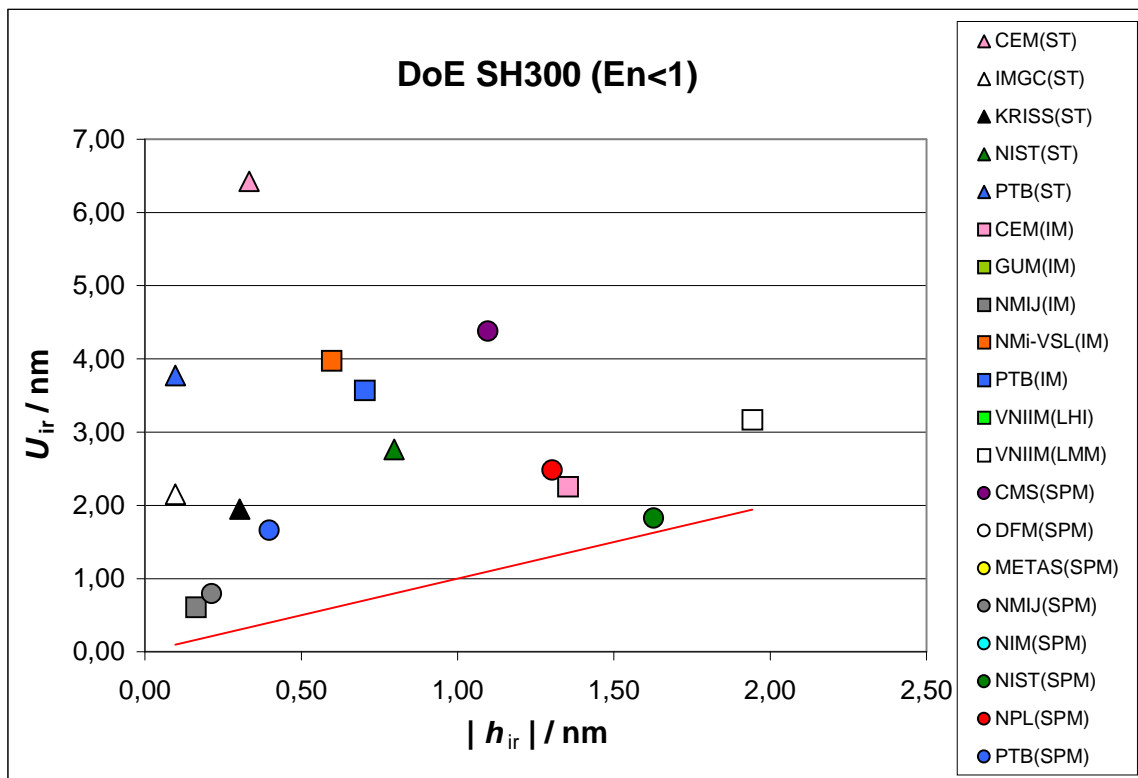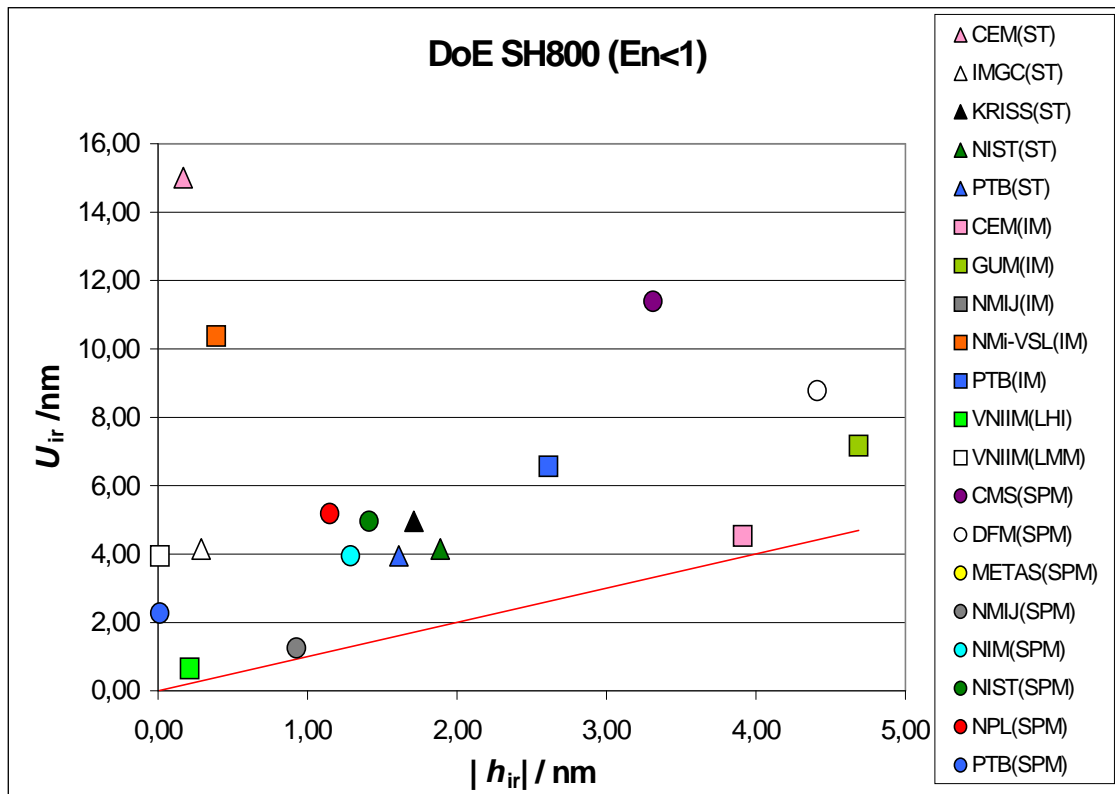
Fig.5.3. Degree of equivalence for the SH070. The U_{ir} values are plotted as function of the absolute deviation from the reference value $h_{ir} = h_i - h_{ref}$.

Fig. 5.4. Degree of equivalence for the SH300. The U_{ir} values are plotted as function of the absolute deviation from the reference value $h_{ir} = h_i - h_{ref}$.

Fig. 5.5. Degree of equivalence for the SH800. The U_{ir} values are plotted as function of the absolute deviation from the reference value $h_{ir} = h_i - h_{ref}$.

9.3   COMPARISON BETWEEN DIFFERENT TYPES OF INSTRUMENTS

In this pre-comparison the size of the step height structures was chosen so that height could be measured by different types of instruments. To detect possible differences between these types the mean value of the step height was calculated for each group of instruments. The results are listed in table 7 together with the standard deviation. In fig. 6 the mean values of the step height obtained by the optical instruments (IM) and the scanning probe microscopes (SPM) are plotted as function of the stylus values (ST). Additionally, a least square fit to each set of data points is given. The small deviation of the slope from 1 shows that there is a very good agreement between the different types of instruments.

Table 7. Mean values of step height for Stylus (ST), optical instruments (IM) and scanning probe microscopes (SPM)

Standard	SH007		SH020		SH070		SH300		SH800	
Method	h /nm	s /nm	h /nm	s /nm	h /nm	s /nm	h /nm	s /nm	h /nm	s /nm
ST	6,55	0,30	20,89	0,24	67,6	0,43	291,2	0,5	778,6	1,5
IM	6,25	0,25	20,59	0,46	67,7	1,24	292,0	1,0	778,7	3,0
SPM	6,58	0,53	20,85	0,57	67,6	0,51	290,9	1,1	779,2	2,3

Final Report

Comparison IM and SPM to ST

$$h_{SPM} = 1,00076 * h_{ST} - 0,12$$
$$R^2 = 1,00000$$

$$h_{IM} = 1,00049 * h_{ST} - 0,05$$
$$R^2 = 1,00000$$

Step height IM or SPM /nm

Step height h_{ST} /nm
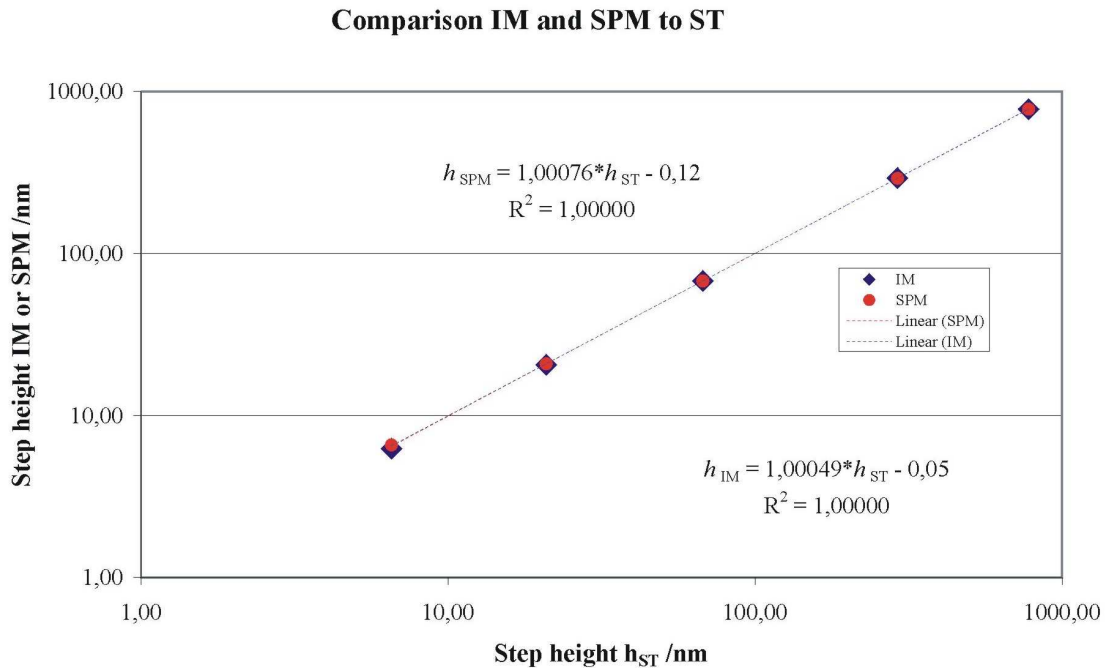
Fig. 6. Mean step heights determined from optical (IM) and scanning probe (SPM) measurements plotted as function of the mean values obtained for stylus instruments (ST)

10 CONCLUSIONS AND REMARKS

The following conclusions are drawn from this comparison:

1.   The comparison was performed within a period of two an a half years. Owing to the good collaboration between the partners, each partner contributed at least one set of measurements. Additionally, an attempt was made to obtain up to date information about the current status of this area of nanometrology. This comparison was the first comprehensive test of the reliability of scanning probe microscopes and their traceability to the SI units in step height measurements since their initial application to dimensional metrology. Consequently, the results of this comparison are of high importance. However, the deterioration of the standards during the comparison show that the number of participants (14) is at the upper limit.

2.   As most results are in good agreement with the calculated reference value the comparison certainly was successful. The comparison also shows that most of participants are able to estimate reasonable measurement uncertainties. The comparison further shows that today step heights on samples can be measured with uncertainties in the sub-nanometer range. Differences in the calculation of the uncertainty depends on the types of instruments and on the user. For each class of instrument, e.g. SPM, it would be meaningful to homogenise the model. Perhaps the uncertainty budget calculations in this comparison could be a good base for this.

Final Report

3.   The definition for "step height" used here (ISO 5436) is more or less a "line height" and the evaluation ranges are too rigid. For the comparison modified ranges were used taking into consideration the restriction of some SPM. For single steps as found on crystalline lattices there is a need for a better definition, too [10] [11].

4.   All participants performed their measurements very carefully and with best detailed knowledge of their instruments. Nevertheless some institutes obtained a different step height value compared to the reference value h_{ref} using the En criteria. Deviation could occur, if an unknown systematic effect had not been considered. Those participants should check their instruments and the uncertainty calculations and make their conclusions accessible, because this information is important for the other participants as well.

5.   Since a set of step height standards was measured, a failure of the En criteria of only one measurement would mean that either the measurement on this standard was wrong or that the uncertainty budget calculation does not consider all contributions in the right way. In the later case this would <u>influence all other measurements of this institute</u>, too, and therefore the other results have to be corrected! This should be taken into account for further comparisons.

6.   Many different instruments (ST, IM, SPM) were used and some laboratories used these techniques for the first time. The comparison of the mean values of the step height for each method shows that for this lateral size of structures and homogenous surfaces there is a very good agreement.

7.   Optical instruments have the advantage of measuring step heights without touching the surface unlike stylus instruments and scanning probe microscopes. The contact techniques could, if performed without appropriate care, damage the sample. Therefore it is necessary for users of stylus instruments to check the force and the stylus carefully in order to avoid scratching the sample under investigation. In the case of SPM it seems that the tip to sample approach often is not performed in a sufficiently controlled way. In the future this should be improved.

8.   For key comparisons it is required that the participants have in house traceability for all quantities which make a major contribution to the uncertainty. In this comparison this is not the case for some participants (see table 3). To check the influence of the correlation to other NMI the uncertainty budget was calculated taking into account this linking. For this calculation we used a correlation coefficient $r_{ij}=1$ or the values given in the calibration certificate. In both cases the change of the uncertainty of the reference value is very small. For example, in the case of the SH20 from $u_c(h_{ref}) = 0,07$ nm to $u_c(h_{ref}) = 0,08$ nm, in the case of the SH800 from $u_c(h_{ref}) = 0,32$ nm to $u_c(h_{ref}) = 0,34$ nm. Also the effect on the En values is small and does not influence the results given above. [12]

---

[10] H. Haitjema, Metrologia, 34 (1997) p. 161 - 167
[11] T. Doi, T. Vorburger, P. Sullivan, Precision Eng. 23 (1999) 135 - 143
[12] En as defined in Eq. 7 and En taking into account correlation effect, too.

Appendix A

Description of the measurement methods and instruments used by the participants

1   CEM 1 - IM –

Description of the measurement methods and instruments

Interferential microscope MicroXAM-Ex from Phase Shift Technology using Phase Shifting technique. This technique, with a very low noise, is adequate for analyzing steps with vertical resolution in sub-nanometer range. For applying this technique the step height difference should be less than $\lambda/4$, λ being the wavelength of the light source. If differences in height was bigger than $\lambda/4$ could have integration errors and hence height measurement errors.

Data:

- Spectral filters for selecting working wavelength. According to the nominal values of the standards we have used the following values:

    - λ_a = 590,6 nm

    - λ_b = 550,5 nm

    - $\lambda_{eq} = (\lambda_a * \lambda_b)/(\lambda_a - \lambda_b)$ = 8 107,86 nm

- Interferometric objectives Mirau type in order to produce interference fringes. Magnifications of X10 and X20.

- Phase shifting in steps of 90º by means of a calibrated piezoelectric.

- Taking of seven to eleven images per phase shift, storing interference fringes.

- CCD camera detecting small changes in intensity level of pixels. Using of these data to calculate step values.

Objectives features:

Magnification	X20	X10
Numerical aperture	0,40	0,25
Measurement area (µm)	422 x 315	845 x 630
Spatial sampling (µm)	1,1 x 1,3	2,2 x 2,6

Temperature during measurements within the range 20 ºC ± 0,2 ºC

Measurement equipment calibrated using several steps/grooves with certified values close to those of the samples to be measured. Measurement results and uncertainty evaluation following GUM document and applying ANOVA method in order to identify and quantify random individual effects.

2   CEM 2 - ST –

Description of the measurement methods and instruments

Stylus profiler **Dektak^3 ST** from Veeco.

Measurement data:

- Vertical Range: 0,001 µm to 6,5 µm
- Vertical Resolution: 0,1 nm
- Scan Length: 90 µm
- Evaluation Length: 70 µm
- Scan Speed: 2 µm/s
- Stylus Tip: Diamond, 2,5 µm radius
- Stylus Tracking Force: 0,05 mN
- Data Points: 7 200
- Horizontal Resolution: 0,013 µm Temperature: 20 °C ± 0,2

Measurement method according to ISO 5436-1 written standard, for steps/grooves type A1. Several significant profiles distributed on each step. Measurement equipment calibrated using several steps/grooves with certified values close to those of the samples to be measured. Before measurements, we proceed to the alignment of the measurement plane of the step with respect to the reference surface, in order to obtain the best internal alignment of all profiles. Measurement results and uncertainty evaluation following GUM document and applying ANOVA method in order to identify and quantify random individual effects.

3   CMS - SPM –

I. Description of the measurement methods and instruments

Step height measurement is taken by an Atomic Force Microscope, which is manufactured by **DI** (Digital Instruments). The model type is Dimension 3100M.

Our step height reference standards is manufactured by VLSI Standards Incorporated (http://www.vlsistd.com) and its model type is STS2-1800S. The surface topography of this standards is shown as in Figure 1, where the height is used. The calibration certificate gives a calibrated step height of 180,0 nm with an expanded uncertainty of 2,1 nm.
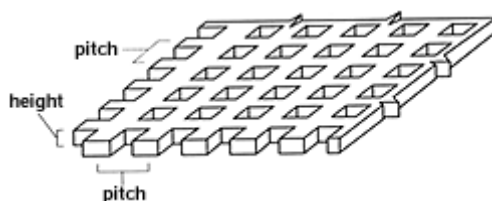
Figure 1. Surface topography of VLSI STS2-1800S standards

For the reference standards, we totally measured 12 times, i.e. 12 images are scanned. The images are then analysed to calculate the step height by using a software called Scanning Probe Image Processor (SPIP), which is established by Image Metrology (http://www.imagemet.com).

For the samples, the area blocked by dashed line is to be measured as shown in Figure 2. The scan size is 70 µm × 70 µm. This area is scanned by AFM to get the image. It is then passed to SPIP software to capture the cross-section profiles at evenly distributed positions on the image as shown in Figure 3. One of the profiles is shown in Figure 4.
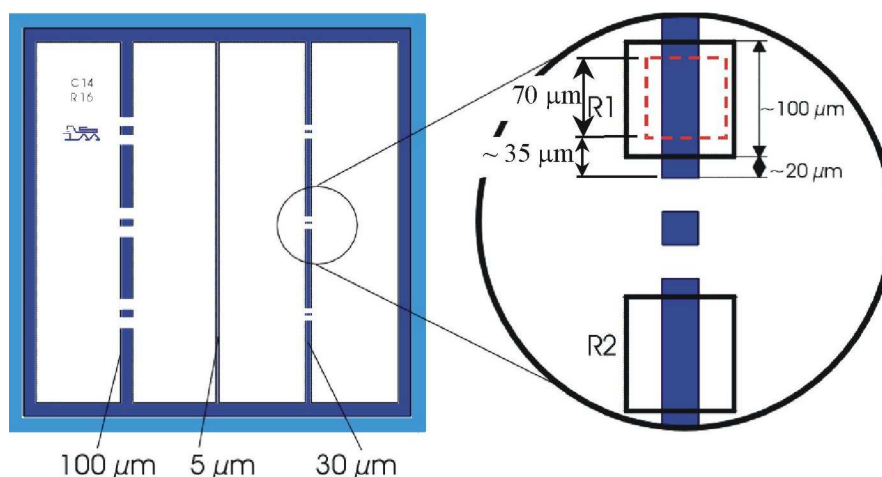

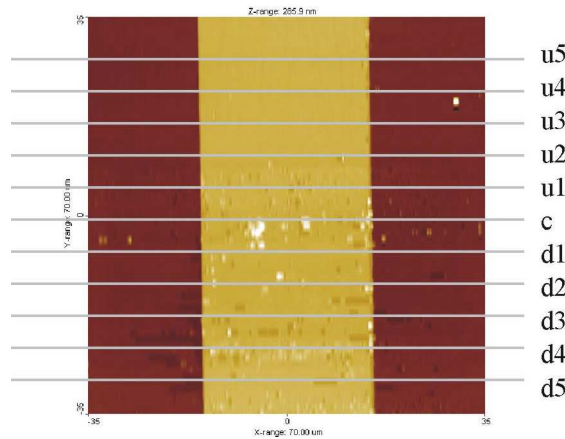Figure 2. The area to be measured is blocked by hidden line

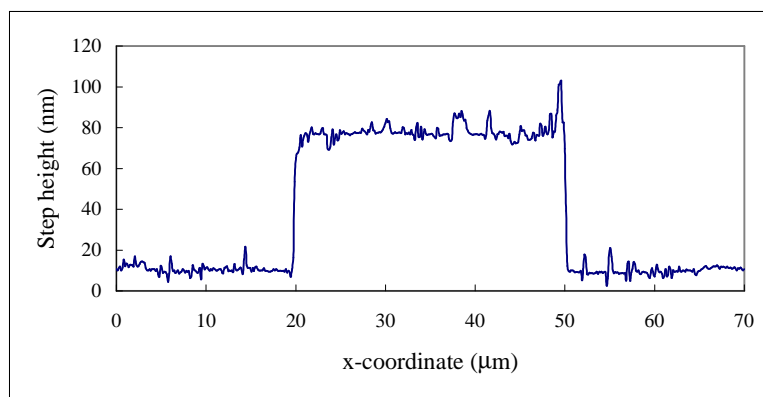Figure 3. Cross-section profiles are taken to estimate the step height

Figure 4. Profile of the step height

The step heights of each profile are then calculated by using a MATLAB program. The algorithm of the step height calculation is stated as below.

As shown in Figure 5, the step height h is defined as the perpendicular distance of the mean of the portion C to the line through the mean of portion A and the mean of portion B.
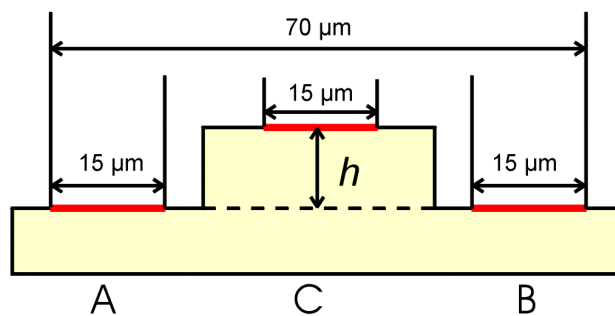

Figure 5. Definition of step height h used in the comparison

The orientation of the captured profile may not be levelled, i.e. the dashed profile shown in Figure 6. If the inclined angle of the line, which passes through the mean of portion A and that of portion B, is θ, the profile can be levelled by rotating an angle of $-\theta$. Then the levelled profile can be found, i.e. the solid profile shown in Figure 6.
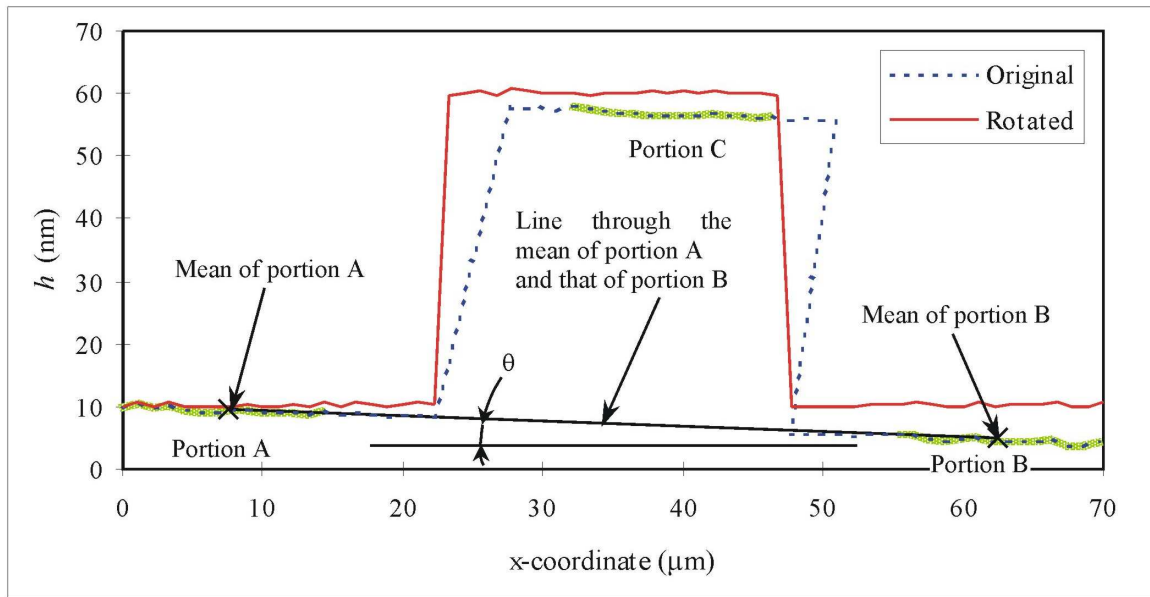
Figure 6. Profile leveling

This rotated profile is used to calculate the step height, which is the difference between the mean of portion C and the mean of portions A and B.

Remark:

Since the sample may be contaminated with dust, defects or scars, the measured profile will not be smooth, such as the profile shown in Figure 4. For each portion, there will be some data that are extremely larger or smaller than the rest of the portion. These are called outliers. Therefore, we have to discard the outliers during the calculation. Outlier can be separated by statistical method. In statistics, quartiles are values that divide a set of observations into 4 equal parts. These values, denoted by Q_1, Q_2, and Q_3, are such that 25% of the data fall below Q_1, 50% fall below Q_2, and 75% fall below Q_3. Interquartile range, denoted by IQR, is the difference $Q_3 - Q_1$. Thus, outlier is defined as the datum that falls below ($Q_1 - 1,5IQR$) or falls above ($Q_3 + 1,5IQR$). Figure 7 shows the schematic diagram of outlier.
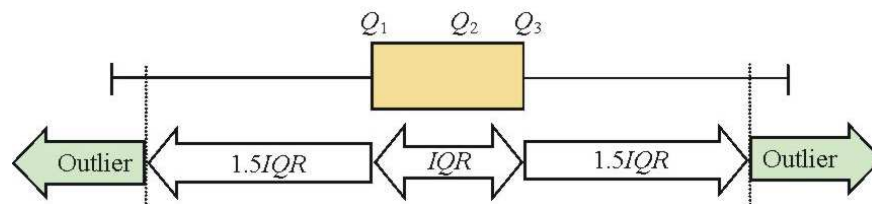

Figure 7. Schematic diagram of outlier

4   DFM   - SPM –

Description of the measurement methods and instruments

A metrological atomic force microscope (AFM) with a scan area of 70 µm × 70 µm × 6 µm, equipped with capacitive distance sensors [1], was used. Measurements were done in tapping mode using silicon cantilevers [2]. Except when mentioned the programme SPIP [3] was used for all image processing.

To calibrate the z-scale a step height was used [4,5]. It had a nominal height of 800 nm, and a nominal width of the step height of 20 µm. It is made in silicon and silicon oxide and covered with a metallic layer of PtIr. It was calibrated by fringe evaluation in an interference microscope by PTB [6]. To estimate the critical out of plane motion for the tip movement a flatness reference were used [7,5]. It is made of a thick piece of super-polished glass covered by chromium. A complete description of the calibration, subdivision and correction of the z-scale is given in [8].

The step height was evaluated at four different spots S1, S2, S3 and S4 along the step height in the square R1 (see **Figure 1**). On each spot two to four images were recorded with the same tip. The measurement on the spots was repeated three or four times with different tips called measurement cycles. The average step height for the four spots was then calculated and the average step height, that is the measurand, is calculated as the average step height for the four different positions. This procedure will take into account the variation of the step height over the measurement area.

The step height is evaluated from images of 64 lines with 512 points, with the edge parallel to the y-axis. A least squares fitted first order line was subtracted from each recorded line to eliminate thermal drift, and an average profile were then calculated. A special developed software algorithm identified the edges of the step and fitted two parallel lines, one line to the profiles A and B segment and the other line to the C segment of the profile (see **Figure**
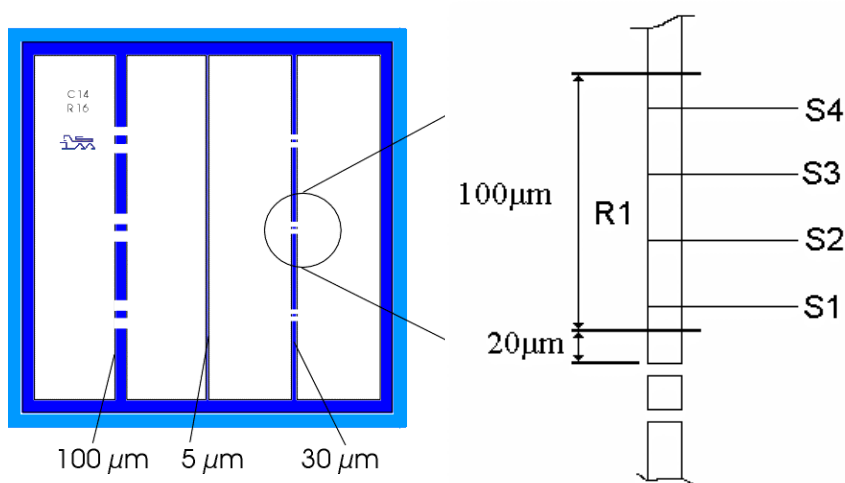

Figure 1. The approximate position of the four spot S1, S2, S3 and S4 where the height is evaluated. From the technical protocol annex A3-Surface Quality Report.

2). The z-coordinate distance between the two parallel line, averaged over the square R1, is then the estimate of the step height h, which is the measurand of the comparison.

Exact calculation

Let $z(x_i)$ be the observed z-coordinate, averaged over the 64 lines in the image, as function of the x position with pixel number i. Let a and b be parameters which removes the tilt and offset of the average profile. Let A, B and C be the segment of the profile to be used for the evaluation according to the Technical protocol (see **Figure 2**). These segments of the profile were calculated from the position of the edges of the steps. The position of the edges was found as the closest x position to the intersection of the profile and an average straight line. The difference in z-coordinate Δz_o for the top and bottom part for an average profile is then fitted from

$$\min_{a,b,\Delta z_o}\left(\sum_{x_i \in C}(z(x_i)-ax_i-b-\Delta z_o)^2 + \sum_{\substack{x_i \in A \\ x_i \in B}}(z(x_i)-ax_i-b)^2 \right)$$

Let $\Delta z_{o\ isc}$ be the observed difference in z-coordinate Δz_o estimated from the average profile for image i, recorded on spot number s, in measurement cycle c. The estimate of
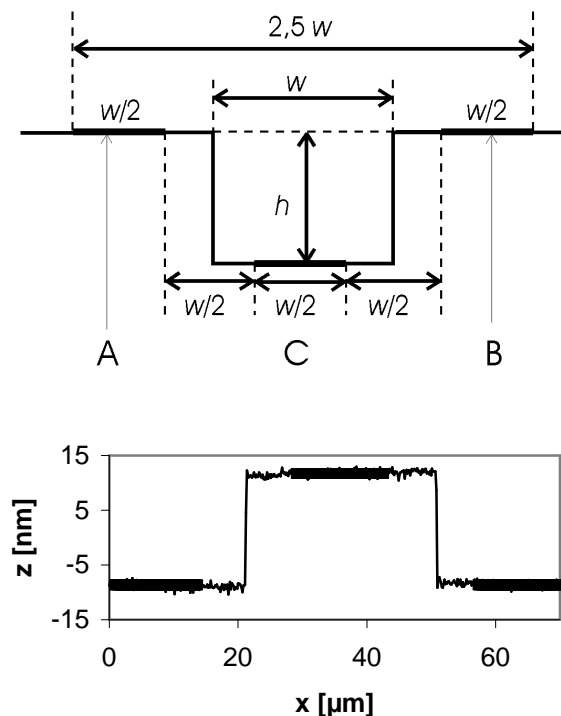

Figure 2. The top is the definition of the step height from the Technical protocol. The bottom is the interpretation of the definition for an average profile. The solid lines is the three parts of two parallel lines fitted to the profile in the three segment A, B and C .

the average observed difference in z-coordinate $\overline{\Delta z_o}$ of the area, is then calculated from

$$\overline{\Delta z_o} = \frac{1}{n_{is}}\sum_c\left(\frac{1}{n_{ic}}\sum_s\left(\frac{1}{n_{sc}}\sum_i \Delta z_{o\,isc}\right)\right)$$

where n_{is} is the number of measurement cycles on spot s, n_{ic} is the number of spots investigated (that is four) and n_{sc} is the number of images on spot s in measurement cycle c.

Let h_{ref} be the reference height of the nominal 800 nm step height and $h_{obs,\,ref}$ be the observed height of the reference. The correction factor C_z, by which the observed height shall be multiplied, is then

$$C_z = \frac{h_{ref}}{h_{obs,\,ref}} \quad .$$

The estimate of the average step height $\overline{h_b}$ of an area is then calculated from

$$\overline{h_b} = C_z \overline{\Delta z_o} \quad .$$

Uncertainty evaluation

To evaluate and explain the uncertainty of the input quantities the auxiliary z-coordinate $\overline{z(A)}$, $\overline{z(B)}$ and $\overline{z(C)}$ is defined as the average z-coordinate of the segment A, B and C of the profile (see **Figure 2**). The difference in z-coordinate $\Delta z_{obs}'$ for the profile segment A, B and C is then

$$\Delta z_{obs}' = \left(\overline{z(C)} - \frac{\overline{(z(A)} + \overline{z(B))}}{2}\right) \approx \Delta z_{obs}$$

The estimate of the measurand is the estimate of the average step height $\overline{h_b}$. The average step height step h of the area R1 is

$$h = \overline{h_b} + \delta z_r + \delta z_d + \delta z_c + \delta z_t + \delta z_l$$
$$= C_z \overline{\Delta z_o} + \delta z_r + \delta z_d + \delta z_c + \delta z_t + \delta z_l$$
$$= \frac{h_{ref}}{h_{obs,\,ref}} \overline{\Delta z_o} + \delta z_r + \delta z_d + \delta z_c + \delta z_t + \delta z_l$$

where

- $u(\overline{\Delta z_o})$ is the difference between the average step height and the fit due to errors caused by
    - the limited number of pixels, and recorded lines

- o the limited accuracy when removing the tilt and offset by the parameters a, and b

- o imperfections in horizontal alignment of the grooves in the image before the average profile is calculated

- o imperfections in estimation of the edge position and there by the A, B and C segment of the average profile

- δz_r is the difference between the observed average step height and the average step height of the area R1 due to roughness and lack of uniformity of the surface and the fact that step height is only probed in selected spots.

- δz_d is the random change of $\overline{z(A)}$ and $\overline{z(B)}$ relative to $\overline{z(C)}$ due to (mostly thermal) drift. The uncertainty $u(\delta z_d)$ will be smaller as the number of uncorrelated measurements increase.

- δz_c is the change of $\overline{z(A)}$ and $\overline{z(B)}$ relative to $\overline{z(C)}$ due to (remaining) coupling between the height z and the position x. This coupling is referred to as "image bow", see [8].

- δz_t is the difference in projected step height for the tilted profile segment A, B, and C and the step height *perpendicular* to the surface.

- δz_l is the error due to remaining nonlinearity of the z-scale. This is because the compensation done by the correction factor C_z is not complete.

References

[1] Dimension 3100 SPM with metrology AFM head, Digital Instrument, USA

[2] NCH PointProbes from Nanosensors www.nanosensors.com, Germany

[3] The Scanning Probe Image Processor (SPIP) from Image Metrology www.imagemet.com, Denmark

[4] H800, made by Nanosensors www.nanosensors.com, Germany

[5] *Nanometre scale transfer standards*, J. Garnaes, N. Kofod, J. F. Jørgensen, A. Kühle, P. Besmens, O. Ohlsson, J. B. Rasmussen, P. E. Lindelof, G. Wilkening, L. Koenders, W. Mirande, K. Hasche, J. Haycocks, J. Nunn, M. Stedman, Proceedings for euspen 1st international conference and general meeting of the european society for precision engineering and nanotechnology, Edited by: P. McKeown, J. Corbett et al., on May 31st - June 4th 1999 Congress Centre Bremen, Germany, Vol 2, 134-137 (1999)

[6] PTB certificate 146 PTB 99

[7] FLAT, made by Nanosensors www.nanosensors.com, Germany

[8] *Calibration of step heights and roughness measurements with atomic force microscopy*, J. Garnaes, N. Kofod, A. Kühle, C. Nielsen, K. Dirscherl, L. Blunt submitted to Precission Engineering June 2001.

5 GUM   - IM –

Description of the measurement methods and instruments

In the Central Office of Measures GUM for "WGDM-7 Preliminary Comparison Nano2 – Step Height Standards" the measurements were performed on the following standards: 20 nm, 70 nm and 800 nm.

According to the requirements of the Technical Protocol the measurand was the average height obtained from different measurements within the reference area R1. For the each standard were performed measurements several times in n sections ($n = 11$), at evenly positions along the step. Also the step depth h was defined according to the requirements of the Technical Protocol.

The typical Linnik's microinterferometer (interference microscope type MII-4) with automatic fringe evaluation was used for these measurements. The green light ($\lambda = 536{,}6$ nm) was applied and additionally – the white light – for the determination of the number of whole fringes of 800 nm standard.

The MII-4 microinterferometer designed by Linnik bases on the schema of the Michelson interferometer. It is adapted to measurements with large magnification (about 500x) in white light or by using the yellow or green interference filter for visual assessment, measurement and photography of the height of grooves on very smooth surfaces. An application of a CCD camera and computer system with "Fringe Application for Roughness Measurement – FringeApp" software has allowed to provide automatic analysis of the interference fringes. The modification of the microinterferometer was performed jointly by GUM and Institute of Micromechanics and Photonics, Warsaw University of Technology.

This microinterferometer is modified by application of:

- fibre optic to illumination of green filter ($\lambda = 536{,}6$ nm),

- phase shifter module integrated with the interferometer base,

- interferogram acquisition module with imaging system and CCD camera (8 bit, 512 x 512 pixels),

- automatic fringe pattern analyser - FringeApp and fitSurf software.

The microinterferometer is supplied with white light source (by using of optical fibre) and green interference filter. On the output of the microinterferometer the additional objective images the interferogram at the CCD matrix. The images are converted by frame-grabber into digital form and stored in computer memory. The automatic analysis of interferograms is performed by temporal phase shifting method. This method requires capturing and analysis of at least three phase-shifted interferograms. The phase shift (every $\pi/2$ – for five phase-shifted interferograms) required is realised by the phase shifter (a step motor and

Final Report

drivers controlled by PC) moving the objective of the microinterferometer, which is near by measured sample.

The automated fringe pattern analyser (with fitSurf software – best fitted plane or 2-nd order surface subtraction) is responsible for controlling the acquisition of the sequential interferograms and enables determination of phase fringes Φ mod(2π) which includes the direct information about surface shape.

The intensity distribution in these interferograms can be described as:

$$I_i(x, y) = a(x, y) + b(x, y) \cos\left[\Phi(x, y) + \delta_i\right]$$ (1)

where:

$a(x,y)$ – is the background intensity distribution,

$b(x,y)$ – is the amplitude of contrast modulation,

(x,y) – the co-ordinates at the detector plane,

$\Phi(x, y) = \dfrac{4\pi}{\lambda} \cdot w(x, y)$ – is a phase to be determined,

λ – is the wavelength of the source illumination,

$w(x,y)$ – is the function describing the shape of measured surface,

δ_i – is the value of relative phase shift between the measured surface and reference beams for the ith exposure.

These five frames of intensity are then combined point-by-point to determine the phase of the wavefront reflected from the measured surface to the reference surface (the mirror' s surface in the interferometer) as imaged at the detector. The phase of the object's displacement $\Phi(x,y)$ at the point (x,y) is given by

$$\Phi(x, y) = arc\,tan\left\{\frac{2\left[I_2(x, y) - I_4(x, y)\right]}{2I_3(x, y) - I_5(x, y) - I_1(x, y)}\right\}$$ (2)

where: I_1, I_2, I_3, I_4 and I_5 are given by Eq. (1) with $\delta_i = -\pi;\; -\pi/2;\; 0;\; \pi/2; \pi$.

Once the phase is determined, the surface heights are linearly related to the phase using

$$w(x, y) = \frac{f \cdot \lambda}{2}\left[\frac{\Phi(x, y)}{2\pi}\right].$$ (3)

Final Report

In relation (3) an aperture correction f of the objective lens used is equal 1, because the microinterferometer MII-4 has two microobjectives. For such microinterferometers the aperture has not practically an influence on the value of interference fringe, equal $\lambda/2$.

The introduction of the CCD camera and imperfect interferometer optics cause a deformation of wavefront, and that has an influence on the obtained phase map of the measured surface. This error is removed by the subtraction the phase Φ_{ref} of the best fitted plane to the very smooth and flat surface of optical flat (the reference plane) from the obtained phase Φ. This is the subtraction of two topographies. Both topographies are the result of an interference evaluation.

Then the shape of the measured surface w_m is

$$w_m = w - w_{ref} = \frac{\lambda \cdot f}{2}\left[\frac{\Phi - \Phi_{ref}}{2\pi}\right],$$

(4)

where:

w − the obtained deformed shape of measured surface,

w_{ref} − the calculated reference plane,

$f = 1$.

The field of view of the measuring system for 33,4x objective was 0,20 mm x 0,14 mm. The vertical resolution was 0,5 nm.

The mean value of the interferometrically measured step height h for $n = 11$ sections of the step is

$$h = \kappa \cdot \frac{\lambda}{2} \cdot f + \overline{h_m} + \sum_j \delta h_j$$

(5)

where:

κ − integer number of fringes,

λ − wavelength of light,

f − aperture coefficient; in this case $f = 1$,

$\kappa \cdot \dfrac{\lambda}{2} \cdot f = h_g$ − integer number of fringes, height in nm,

$\overline{h_m}$ − mean height of measured step (only fraction of fringe) obtained as a result of sections (for $n = 11$) of the measured surface w_m (m − repeated observations), height in nm,

$\overline{h_m} = f(\lambda, f, \Phi, \Phi_{ref}, n, m)$

δh_j – corrections:

δh_{noise} – noise in the system (with intensity influence of illumination),

δh_{foc} – de-focus,

δh_R – roughness influence,

δh_{phd} – difference of phase by material difference,

δh_{nl} – non-linearity of the phase shifter; interference evaluation,

δh_{dig} – digitisation (512 pixels),

δh_p – profile evaluation

6   IMGC   - ST -

Description of the measurement methods and instruments

The step-height standards have been measured at IMGC using a stylus profilometer (Talystep 1, Taylor Hobson- RTH). The instrument works with a PC control (RTH Talystep PC software 0,01 SP) for data acquisition, calibration and setting of measurement parameters. The surface profiles have been analysed using the software RTH – Groove (3.02P IMGC), which calculates the step-height according the ISO 5436.

The instrument has a traverse scan range of ~2 mm and a measuring pick-up vertical range of ~12 µm at the lowest magnification, down to a range of ~30 nm at the highest magnification. Since at this high magnification, vibration, acoustic noise and thermal drift may seriously affect measurement results, our instrument is placed on a massive table with inner air tubes for vibration isolation, in a room with air temperature control. In addition, the instrument itself is equipped with an antivibration base platform and is placed in a insulating box.

Talystep 1 has been calibrated by means of displacement piezo-capacitive transducers (DPT-10 from Queensgate) which , in turns, have been calibrated using a heterodyne interferometer, namely by sampling the displacements of the transducer at steps of $\lambda/4$ in order to minimize the non-linearity error of the interferometer. By correcting the observed non-linearity of the transducer, the resulting expanded uncertainty of the transducer displacements is thus estimated as $0,7nm + 1 \cdot 10^{-4} \cdot d/nm$.

By driving the DPT with a low-frequency square-wave AC signal we produced corresponding vertical displacements of the Talystep pick-up in contact with an optical flat mirror glued to the moving part of the transducer. In this way, the pick-up vertical displacements resulted in a recorded profile having a rectangular shape and a definite step height. The profilometer has been calibrated driving the DPT at square-wave displacements from 7 nm up to about 800nm. As a further test, the Talystep 1 was checked with a certified groove standard (RTH calibration specimen 112/964).

All the measurements on the circulating standards have been taken with the profilometer in the unfiltered mode, pick-up traverse speeds of 2,5 and 25 µm/s, a sampling length of 100 µm, with which the data sampling interval is of ~ 0,1µm. A stylus tip having a pyramidal shape with angles at the vertex from 90° to 120°, truncated to nominal radii of 0,2 x 2,5 µm, has been used. The stylus is mounted so that the larger dimension of the tip is perpendicular to the direction of pick-up traverse movements. The stylus loading has been adjusted from 10 µN up to 35 µN, respectively for the step-height standards from 7 nm up to 800 nm nominal steps.

The specimens have been measured at several sampling points (>5) spaced of about 20 µm, forth and back along the reference area (R1). The xy-stage of the instrument has been used for levelling and positioning the sample. The measurements have been taken at a room temperature of $(20 \pm 0,3)$ °C.

Final Report

The sample SH07 (C17 R21) has been measured at several sampling points (>10) because in many of them the recorded surface profiles showed a convex shape at one side of the step. Such a shape has been observed traversing forth and back the step, and we believe it is not due to some instrumental error. Nevertheless, the convex shape at one side of the step was not observed in few other sampling points of the reference area R1. Therefore, for the SH07 we decided to give the average step obtained from these last sampling points where the profiles are regular. In addition, the average step obtained from the profiles taken in all the sampling points is given within brackets.

7   KRISS - ST –

Description of the measurement methods and instruments

Stylus instrument (Nanostep 2, Taylor Hobson Ltd., UK), which is installed in the constant temperature room (temperature regulation: 19 - 21°C), was used for the step height measurement. The larger steps (SH 800, 300, 70) were measured in the stylus gauge range1 where the vertical displacement up to 20 μm can be measured with the resolution 0,3 nm, while smaller steps (SH 20, 7) in the 10 times more sensitive range 2 (2 μm / 0,03 nm). The stylus tip radius, stylus force and the traverse speed were 2 μm, 5~7 mgf (50~70 μN) and 0,1 mm/s, respectively throughout the measurement. The two step height masters, each with the certified value of (940,2 ± 4.5) nm and (96,84 ± 0,50) nm, respectively, were used to set the calibration constant of stylus gauge range 1 and 2. The step heights of two masters had been calibrated with Nanostep in the Gauge Range 1 after calibration by means of step gauge whose step height is determined as (5,0656 ± 0,0022) μm with the gauge block interferometer at KRISS. For each of the specimens SH 800, 300, 70, the .two sets of measurements was done in the gauge range 1, while the third set in the gauge range 2. The first set includes 5 traces over the area R1, and the second and third set 9 traces. For the specimen SH 20 and 7, the measurements were done in the range 2, one set for SH 20, and the two sets for SH 7. Each set equally includes 9 traces. The uncertainty components considered includes:

1)   The uncertainty from height masters H and L used for the calibration of gauge range 1 and 2, respectively.

2)   The combined uncertainty from the uniformity of the reference specimen and instrument repeatability in the calibration (random_C).

3)   The combined uncertainty from the uniformity of the specimen and instrument repeatability in the measurement (random_M).

4)   Non-linearity of the transducer in the Gauge Range 1. In the Gauge Range 2, it was neglected since the instrument does not show any consistent tendency.

8   METAS - SPM –

Description of the measurement methods and instruments:

An AFM profiler system consisting of a linear long range sample displacement stage and a commercial metrology AFM head (Digital Instruments) was used for the step height measurements. The linear displacement stage moves the sample up to 380 µm horizontally while the AFM head probes the surface with a sharp silicon tip and measures the local height. An optical zoom video microscope and a coarse x-y table allow an easy positioning of the location of interest below the tip (Fig. 1).
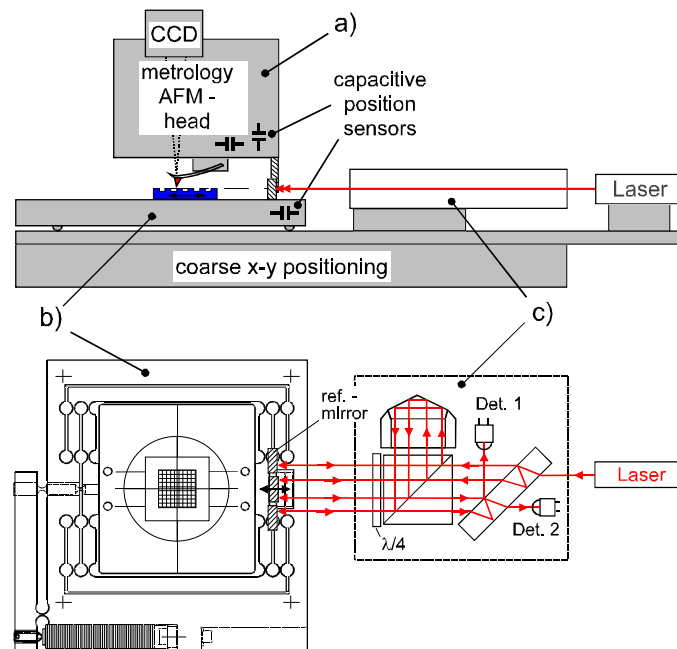

Figure 1. General setup of the long range AFM profiler system. a) metrology AFM head including a video microscope, b) piezo actuated linear long range displacement stage with monolithic flexures forming a double parallelogram and c) schematic of the differential double pass plane mirror interferometer with HeNe-laser.

The linear long range displacement stage consists of monolithic flexures forming a double parallelogram and is piezo actuated. The position is adjusted by a 21 bit DSP controller using a capacitive position sensor signal for the feedback [1].

The z-position of the AFM tip is measured by a capacitive position sensor inside the AFM head. The calibration of this sensor was made in two ways: a) by using a piezo driven tilting device and b) interferometrically by using a 90°-deflection prism.

a) The tilting device was placed on top of the linear displacement stage maintaining the sample surface at the height of the rotation centre (Fig. 2a). Through an x-displacement of the linear stage, an accurate z-motion of the sample surface is generated. The z-calibration is done by recording the z-sensor signal versus the x-displacement of the stage at two or more angular positions using a sample with a smooth surface. As the z-displacement is generated at the place of the tip, there is no Abbe offset involved in this method. Influences due to an imperfect straightness of the linear stage motion or due to a rough sample are partly canceled out by the fit applied to the measured profiles. The tilting device allows for four angular increments which were calibrated with our national standard for angle.

Final Report

b) The setup for the direct interferometric z-axis calibration method is shown in figure 2b. Here a mirror was fixed under the AFM tip. A 90°-deflection prism below the scanner is used to deflect the two laser beams of the differential plane mirror interferometer into the vertical direction. The reference mirror of the differential interferometer is attached to the linear displacement stage. X-movements of the stage with respect to the AFM head are therefore cancelled. For both methods the average z-sensitivity calibration was finally better than 0,05% [2].
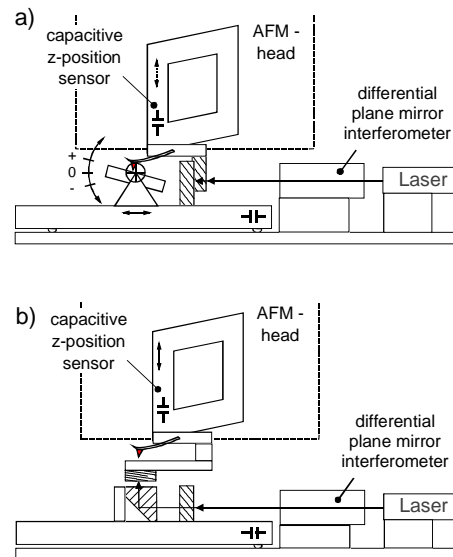

Fig. 2. General setup of the two height calibration methods. a) using a piezo driven tilting device and an interferometrically measured lateral displacement, b) direct interferometric z-axis calibration with an 90°-deflection prism.

The measurement strategy:

The AFM was always operated in tapping mode. To reduce the effect of drift always a pair of trace and retrace profiles were evaluated together. On each sample 15 profile pairs, distributed equally over an area of 70 µm x 70 µm in the centre of the measurement field R1 were acquired. The profiles were measured over a length of 110 µm with 1 point per µm data spacing. For each profile the evaluation was made on the central 70 µm with subranges for the upper and lower part of the ridge according to the instructions (3 x 15 µm). Two lines were fitted through the corresponding ranges and the local height was calculated to be the distance of the two lines at the centre of the ridge. To reduce the influence of impurities only profile data points within two sigma were used for the line fitting. Finally the step height is given as the average of all 15 local height pairs (see evaluation illustrations in the attachment).

The uncertainty budget contains 7 main influence quantities: Repeatability, linear and nonlinear z-calibration of the AFM head, scanner flatness, temperature deviation, uniformity and roughness of the standards. The largest contributions to the total uncertainty were the scanner flatness and the uniformity of the standards. Only for the largest step height of 800 nm the z-calibration becomes more important. The widths of the ridges are with 30 µm quite large for an AFM calibration sample. For smaller widths or if only the left or the right side of the ridge would be used for the definition of the step height the scanner flatness term would be much smaller.

The roughness was also influenced by impurities present on the surface of the standards. Illustrations are included on separate pages (Optical dark field images of the samples in the "as received" state before the METAS measurements, 3D AFM topographies and typical profiles for all samples.)

References:

[1] F. Meli and R. Thalmann, Measurement Science and Technology, **9**, 1998, p. 1087-1092

[2] Measurement Science and Technology, **9**, 1998, p. 1087-1092)

Comment from METAS to its results (Dec. 11, 2002)

METAS has measured all five stepheights. The results for the three lower steps seem to be fine while the there is a very clear problem with the results for the two larger steps (290 nm and 780 nm). The AFM head seems to have had a defect which did not show up in the interferometric z-calibration made before and also after the comparison. The measurements took place in February 2001. At this time several labs at METAS moved to a new building. Therefore other instruments like the stylus profiler and the interference microscope were not available for cross checking the results. Since then the AFM was not used for the calibration of steps larger than 100 nm.

New investigations made since the release of draft A point to the following probable explanation:

The z-stage of the scanner, a piezo actuated parallelogram, seems to have some sort of internal friction. The capacitive position sensor has an Abbe offset of 14,4 mm in y-direction and 12,5 mm in z-direction. The interferometric calibration was made with nominal no Abbe offset with respect to the location of the tip. Therefore repeatable angular errors are to a large part taken into account in the calibration. Influences of the angular error of the z-stage together with some remaining Abbe offset were checked by displacing the interferometer beam out of Abbe. This influence was found to be small.

However, probably due to some internal friction the angular error is not fully repeatable, that means there are some hysteresis and creep effects. As the interferometric calibration was always made over the full z-range in the up or down direction this effect was not discovered. In fact the interferometric calibration gave the same calibration constants since several years. The effect shows up only when a reversal of the z-movement occurs. For small step heights (and small sample tilts) the effect is also small. For this reason the measurements on the small steps were fine. Due to this complicated error source we can not give any correction values to the stepheights measured in February 2001.

We know this problem was not present at earlier times before the comparison measurements were made. METAS will clarify this and repair the head with the highest priority.

9   NMIJ 1 - IM –

1. Step height measurement using interferometric microscope

The samples (SH7, SH20, SH70, SH300 and SH800) were measured using an interferometric microscope with a Mirau-type interferometric objective (20x or 50x, manufactured by Nikon Co. Ltd.) [1]. Figure 1(a) shows the design of our instrument and the mechanism used to directly and absolutely measure the fringe spacing and to measure 3D topography of the sample by the phase-shifting technique. The measurements were carried out through two steps as shown in Figs.1(c) and (b).
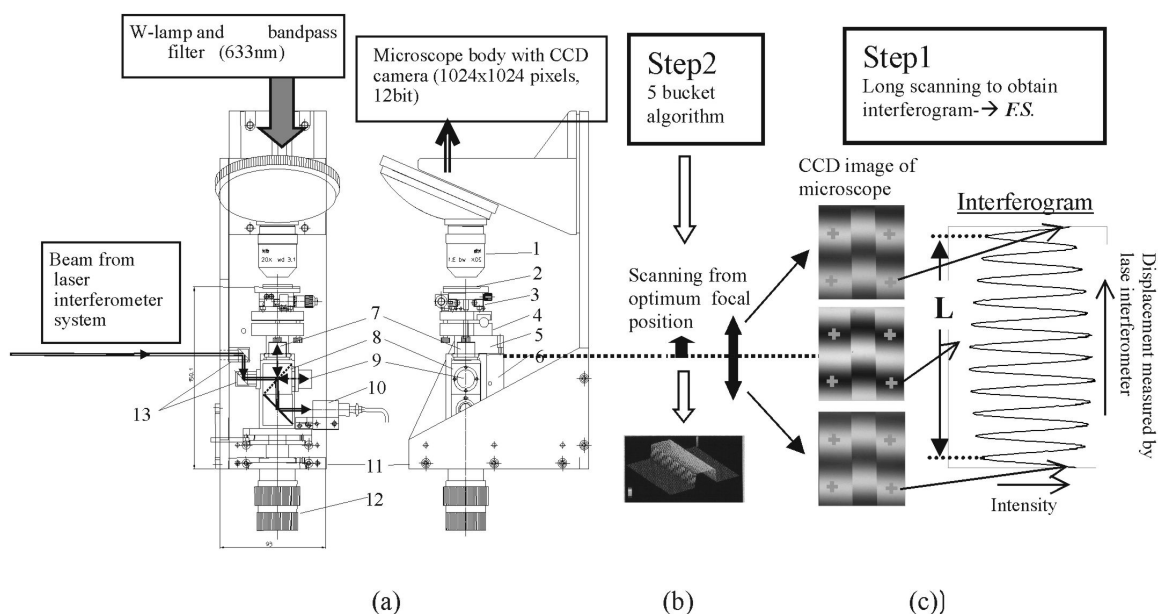

(a)   (b)   (c)

Fig. 1. Apparatus used to measure fringe spacing and 3D surface profile by phase-shifting technique (1: Mirau-type interferometric objective (20x or 50x, manufactured by Nikon Co. Ltd.), 2: sample, 3: X-stage, 4: X-Y tilt platform, 5: scanning base plate, 6: PZT device, 7: corner cube scanned, 8: polarizing beam splitter, 9: corner cube fixed, 10: detector of laser interferometer system, 11: suspended base body, 12: differential micrometer for focusing, 13: beam benders)

In step 1 of Fig. 1(c), the sample is scanned along the optical axis of the microscope by a PZT device (6 in Fig. 1) from +5,25 fringe to -5,25 fringe in the case of a 20x Mirau-type objective. The position of the sample at each point is expressed as the number of fringe shifts with respect to the optimum focal position. A positive number indicates *underfocus* (i.e., the distance between the sample and objective is larger than that of the optimum focal position), and a negative number indicates *overfocus*. During the scanning, intensities at four points of CCD images (indicated by + in Fig. 1(c)) and the sample positions measured using a laser interferometer are stored. For each measurement point of the CCD images, an interferogram (Intensity vs. Sample displacement) can be plotted as shown in Fig. 1 (c). The second-order fitting is applied in the vicinity of each bottom in the interferogram and accurate positions of bottoms are determined. The fringe spacing (**F.S.**) for each point is calculated by

$F.S.$= (Displacement corresponding to 10 bottoms of the interferogram) / 10 = L/10.   (1)

The average $F.S.$ at the four points in the CCD image is determined as $F.S$. It takes 40 seconds to carry out this measurement. The measurement is repeated 3 to 6 times.

In step 2 of Fig. 1(b), the 3D topography of the sample is measured using the phase-shifting technique (5 bucket algorithm). The $F.S.$ measured in step1 is used both as the basic scale of height and as the accurate phase shift value of the phase-shifting technique. By carrying out a similar procedure, the samples were measured by Mirau-type objectives with magnification of 50x.

2. Measurement conditions

The measurable areas (the CCD image area) are 340x340µm^2 and 136x136µm^2 for the 20x and 50x objectives, respectively. Each measurement of 3D topography (by the phase-shifting technique) was carried out under the condition of making two fringes in the CCD image area as shown in Fig. 2. The optimum focal position was defined when the midpoint of the two darkest fringes was placed in the center of the CCD image area except for the area of the step part. The step height (h) value for each sample was determined from the data obtained using the 20x objective. The relationship between the CCD image and R1 area is shown in Fig. 2. There were many dusts on the samples. The dusts were excluded using masks as shown in Fig. 2. For approximate 300 x-line profiles corresponding to R1, the step heights were calculated according to the protocol. The calculated values of step height were averaged and each result was determined as the final value of step height for each sample.

CCD area; 340x340µm^2 CCD area; 136x136µm^2
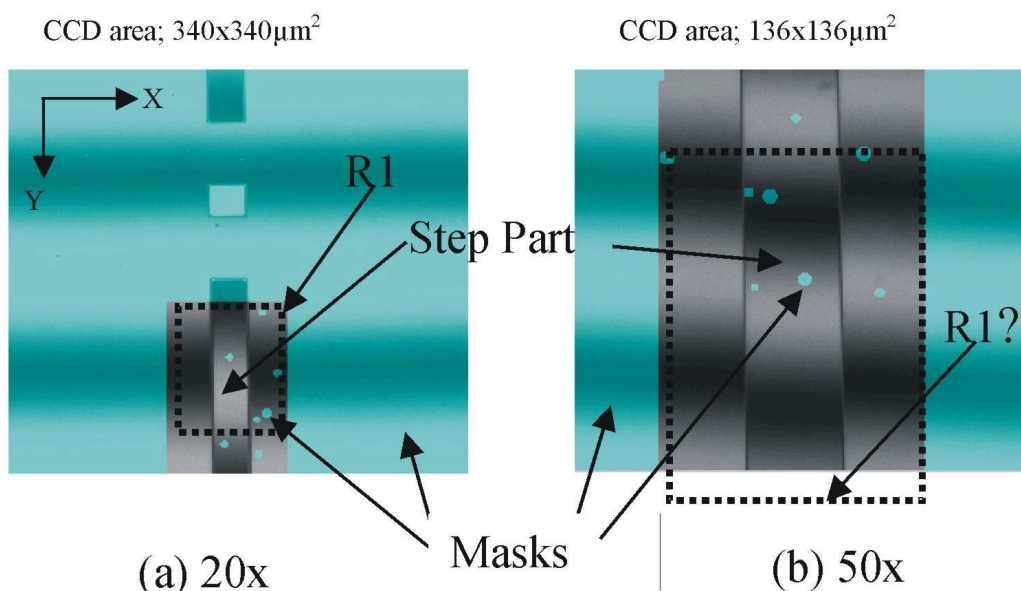
(a) 20x   (b) 50x

Fig. 2. Conditions of step height measurements (interference fringes, focus, step part, R1 and masks in the CCD image area). The masks were used to exclude dusts and the areas which are independent of step height determination.

The area measured by a 50x objective could not always cover the area of R1. We could not finely adjust the sample position in the y direction, because our instrument is not equipped with a Y stage. By analyzing the results obtained using the 50x objective and comparing the results obtained using the 20x objective with the results obtained using the 50x objective, the uncertainties were estimated.

All measurements were carried out under the laboratory conditions of temperature $20,5\pm1°C$ and relative humidity $50\pm5\%$.

3. Analysis of uncertainty

The uncertainty factors are also classified into two types. One type is derived from the determination of the fringe spacing (*F.S.*) measured by the laser interferometer system. The other type is derived from the phase-shifting technique, which yields the 3D topographic image.

3.1 Uncertainty to measure displacement of the sample (*L*)

The laser interferometer used in our instrument is a commercially available one (HP5517C) with the resolution of 1,2nm. The long-term stability (1hour) of laser frequency is $2x10^{-9}$. The accuracy of laser frequency (lifetime) is $3,33x10^{-8}$. The wavelength change by the refractive index of the air was estimated using Edlen's equation on the basis of measured temperature, humidity and pressure. The Michelson interferometer (depicted by 7, 8 and 9 in Fig. 1) is compact and covered by the housing. The dead path of the Michelson interferometer is designed as zero, however a dead path of 0,1mm was assumed. Cosine error and Abbe error were also estimated.

3.2 Uncertainty to determine *F.S.*

To determine *F.S.* using Eq. (1), the hypothesis that the *F.S.*s are uniform from +5 fringe to -5 fringe is required. We measured *F.S.* 45 times and checked the *F.S.* variations from +5 fringe to -5 fringe for each point of each measurement, however no systematic change of *F.S.* was observed. In ref.2, the sample with 90nm step height is measured at the defocus position from +8 fringe to -8 fringe. The change of step height values by defocus comes from the deformation of the base plane or base line. If the appropriate algorithm to determine step height is applied, the change of measured step height value, in other words, the change of *F.S.* at the defocus position, is very small. The uncertainty of the change of *F.S.* (dispersion of *F.S.*) was estimated at 0,145nm.

3.3 Defocus

Two kinds of samples with step heights of 46nm and 940nm were measured from +4 fringe to -4 fringe defocus positions. The step height values were calculated according to the protocol. The step height value change due to the defocus was 0,04nm/fringe for the 46nm step height sample. For the 940nm step height sample, the step height value change due to the defocus was 0,25nm/fringe at the position of overfocus and 0,1nm/fringe at the position of underfocus. For the samples of SH7, SH20 and SH70 and for the samples of SH300 and SH700, sensitivity coefficient of uncertainty due to the defocus was determined at

0,04nm/fringe and 0,25nm/fringe, respectively. The focus adjustment uncertainty was smaller than 0,2 fringe in our setting.

3.4 Uncertainty of phase calculation by phase-shifting technique

The important uncertainty factors in the phase-shifting technique are detector nonlinearity, phase shifter miscalibration (PZT), phase shifter nonlinearity and vibration. The uncertainties listed above are not always independent. In the case of step height calibration, the phase difference between the base part and step part is important, too. Almost all uncertainty factors cause an error at twice the fringe spatial frequency [3]. The phase shifter of our instrument is closed loop controlled using a capacitance sensor. The nonlinearity of the PZT is less than 0,04%. The uncertainty due to the phase shifter is considered to be very small [3]. Vibration is reduced as much as possible by applying a suspended base body (11 in Fig. 1). To estimate the above-listed uncertainty factors, the samples were measured at three focal positions (i.e., the optimum focal position, $\pi/2$ shifted position, and π shifted position) using 20x and 50x objectives. From the discrepancies of the measurements, the uncertainties of phase calculation by the phase-shifting technique were estimated.

3.5 Roughness of reference mirror

Even though the measurement by the 50x objective did not always cover R1 area, identical areas between the results measured by the 20x and 50x objectives could be found. In the identical areas, the discrepancies of step height values were calculated for SH7, SH20 and SH70. The standard deviation of the discrepancies was 0,137nm. From the result, the uncertainty of the roughness of the reference mirror was determined as 0,027nm.

3.6 Identification of R1 area

In our method to identify the R1 area, the uncertainty in the identification of R1 area was ±2,7µm. For each sample, step height change was estimated when R1 area was shifted by ±2,7µm in the y direction.

References

[1] T. Doi and T. Kurosawa: Accurate optical surface profilometer based on Mirau-type interferometric microscope, Proc. of the euspen, p. 462-465, 2nd International Conference, European Society for Precision Engineering and Nanotechnology, May 27th-31st, 2001, Turin, Italy.

[2] T. Doi, T. Vorburger and P. Sullivan: Effects of defocus and algorithm on optical step height calibration, Precision Engineering, Vol.23, p. 135-143, 1999.

[3] K. Creath: Errors in phase-measuring interferometry, Proc. of SPIE, Vol. 1720, p. 428-435, 1992.

10 NMIJ 2 - SPM –

Description of the measurement methods and instruments

1. Measurement

A nanometrological atomic force microscope (nanometrological AFM) with three-axis laser interferometer was used for this comparison. Maximum scan area of the nanometrological AFM in normally servo controlled mode was only 17,5(X)×17,5(Y)×2,5(Z) μm and was not enough to measure the step height samples with 30 μm line-width. The 50(X)×50(Y) μm scan area could be obtained using not a servo controlled mode by interferometer signals but an external high voltage amplifier. Maximum 70 μm scan area could be reached and the step height samples were measured with diagonally stage scanning. The Z-axis scanner was controlled to keep the slope of micro-cantilever in measurement. The position of the XYZ three-sided moving mirrors fixed at the top of the Z-axis scanner was measured and the obtained XYZ interferometer signals were used for the topography image of the step height samples.
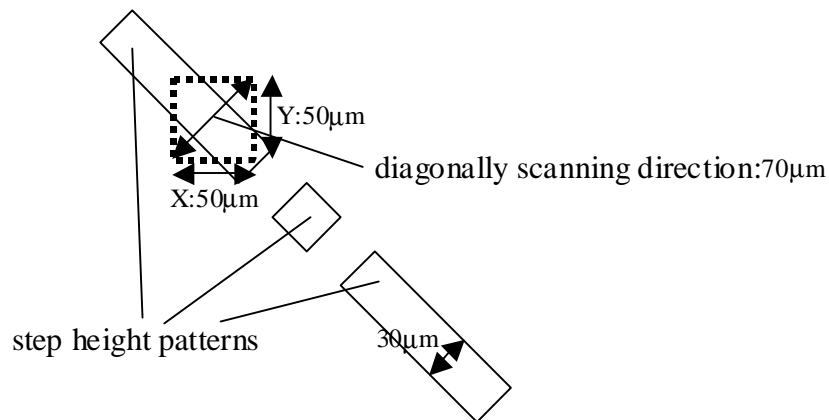

Figure 1. The widened scan area for the measurement of step height samples.

The profiles were taken with a contact mode of AFM. The nominal spring constant of micro-cantilever is approximately 0,01 N/m. 8 measurement points were selected in each sample (SH20, 70, 300 and 800) and 3 points were only taken for SH7. The order was decided at random by a random number table. Maximum 506 step height measured values were obtained in 1 measurement. The scanning speed was approximately 14 μm/sec.

2. Analyses

(1) Laser wavelength

The wavelength of the lasers at every measurement was calibrated using Edlen' s equation with the values of ambient temperature, air pressure and humidity. Other sections in NMIJ-AIST calibrated the sensors measuring these parameters. The frequency of the lasers used in these measurements was calibrated in comparison with that of I_2-stabilized He-Ne laser.

Final Report

(2) Slope correction

The obtained profiles were not surface ones but line ones. X-axis direction scanning and Y-axis direction scanning were done after the measurement of the step height samples, and both slopes were used for the correction of the line profiles.

(3) Correction for the thermal expansion

The thermal expansion of step height samples was corrected to values corresponding to 20°C.

11 NMı-VSL - IM –

Description of the measurement method and instrument

Instrument: Zeiss Interphako interference microscope with phase modulator and digital readout of the phase adjustments.

Measurement method:

Step 1: Determination of the approximate step heights using the zero order fringe in white light by measuring the phase difference between the two images (left and right) of the step.

Step 2: Calibration of the aperture correction of the microscope (objective and illumination system) using a calibrated 2 μm nominal step height standard at the 546,23 nm line of a mercury discharge lamp. The calibration of the 2 μm nominal step height standard was performed using a Form Talysurf profilometer.

Step 3: Calibration of the phase adjustment knob using the 546,23 nm line of a mercury discharge lamp.

Step 4: Determination of the phase delay of the step heights using the 546,23 nm line of a mercury discharge lamp. Each standard was measured at 5 different locations within the measurement field R1. Each measurement consists of 10 individual data points.

Step 5: Calculation of the step heights and associated uncertainties

12 NIM - SPM –

Description of the measurement methods and instruments

The instrument used in the measurement is a metrological atomic force microscope(AFM) which consist of two main part. One is the AFM VERITEKT 3 used for the measurement. And another is a integrated macro three dimensional interferometer system used for the calibration of scanner of AFM. The measuring range of AFM is (x, y, z)=(70, 15,15) μm. And the resolution is (x, y, z)=(1,25; 0,25; 0,25) nm.

There are a lot of error sources that have influences on the budget of measuring uncertainty. Those error sources list as follow:

1: error of laser wavelength

2: measuring uncertainty of interferometer

3: residual error of scanner calibration

4: the influence of temperature.

5: surface roughness of standard

6: pollution of surface of standard

7: the change of surface hardness

8: property of elasticity and plasticity of material on surface

9: capillary force rising from water layer on surface

10: Van der Waals force.

The maximum step height is 800 nm, therefore the error of wavelength can be neglected. The influence of temperature can also be neglected too because of same reason (another reason is to calculate the step height of each measuring line and that there is no temperature index of material of standard in the document). It is very difficult to determine the value of item 5 to 11, which can be got neither by means of measurement nor from experience data and references. Therefore we evaluate these items in the distribution of measurement.

Before the measurement of step height standards, we had done the calibration of scanner. It shown that the residual nonlinear error in z direction ztz is small than 1 nm and the residual cross-talk error in z direction when x axes moving xtz is small than 2nm.

Because the moving range is 15μm and measuring range required in the Technical protocol of Nano 2 is 100μm in y direction, we made the measurement at three positions (top, middle bottom) on this area with one setting. The measuring area is (x, y) =(70, 12) μm and the measuring points is (x, y) =(400, 200). The deflection of cantilever is 15 nm. Each standard has been measured three times in this way.

The calculation method is:

1: selecting suitable area in the map picture of measuring data to calculate the step height of each measuring line;

2: getting average value from all of those step height values of single lines as the result of a single measurement.

3: the final step height is the average of all the values of the single measurements.

13 NIST 1 - SPM –

Description of the Calibrated Atomic Force Microscope and the measurement methods used

The step heights of five Nano2 specimens were determined from measurements performed using the NIST calibrated atomic force microscope (C–AFM), shown in Figure 1. The C–AFM is a custom-designed AFM for dimensional metrology, primarily for the calibration of physical standards for other AFMs. The C-AFM has metrology traceability via the 633 nm wavelength of the I_2-stabilized He-Ne laser (a recommended radiation for the realization of the meter in the visible) for all three axes. This is accomplished using heterodyne laser interferometers. The C–AFM employs a scanning-sample design. A piezoelectrically driven two-axis flexure stage, with a nominal 100 µm range, is used to translate the sample in the x- and y-directions. It has small straightness and angular motion deviations. Heterodyne laser interferometers monitor the x-y displacement, and a digital signal processor in the controller is used to allow closed loop control of the lateral sample position. This eliminates the scale calibration and linearity problems of the scanners used in most commercial instruments.

The vertical (z) position of the sample is driven with a piezoelectrically actuated, flexure-guided transducer with an integrated capacitance sensor. In Fig. 1, this package is called the z-stage. The z-stage provides one axis of rectilinear motion with very small straightness and angular errors, and the internal capacitance sensor provides measurement of the z-stage extension with high repeatability and high resolution. To achieve traceability, this sensor must be calibrated using a third interferometer. This is done by removing the AFM sensor and inserting a z-interferometer in its place, then comparing the capacitance gauge signal to the z-interferometer signal for the same range of vertical displacements. The system is calibrated in this way each day that the C-AFM is used for measurements. After the z-stage calibration is complete, the z-interferometer is removed and the AFM sensor is re-inserted to perform height measurements. The system can be operated with several AFM heads, allowing operation in both contact and intermittent-contact modes as well as allowing the use of both optical-lever force sensors and piezo-resistive cantilevers. Low thermal expansion materials and kinematic mounts are used to minimize drifts in the sensitive components of the system, and the instrument is operated in a temperature-controlled laboratory with stability of 0,1° C.

All specimens were characterized using the basic measurement plan shown in the Nano2 instructions whereby an area of the step standard about 85 µm long and 70 µm wide was measured. Each measurement of step height is derived from topographic areal data consisting of approximately 250 profiles each containing about 2000 data points. Each topographic image was inspected by eye for profiles containing bad data, perhaps arising from surface particles or noise transients. Profiles with bad data were excluded from the analysis.

Sources of uncertainty

A number of sources of uncertainty must be taken into account for measurements of all five step heights. The general uncertainty budget for the C-AFM for measurements in the z-direction has been published elsewhere [1,2]. That uncertainty budget was refined and

rechecked for the specific conditions of the Nano2 measurements. Each component of uncertainty is briefly described below.

Repeatability of the measurement of step height
Numerous sources of noise in the measured profiles cause variation in the measured results. These are accounted for in most cases by taking repeated topographic images, calculating the average step height for each image and then calculating the standard deviation of the mean of the results.

Capacitance gauge calibration, reproducibility
This is one of several components of uncertainty arising in the calibration of the capacitance gauge by interferometric displacement measurement over a height range of approximately 1 μm. This procedure is performed each day that the capacitance gauge is used for step height measurements. The calibration procedure yields a value for the sensitivity of the capacitance gauge that is approximately 3,596 nm/mV, but which varies from day to day. One source of the variation is the polarization mixing of the interferometer, which varies in amplitude and phase from day to day. We assume that reproducibility in the measured capacitance gauge sensitivity could lead directly to variability in the measured step height and we therefore include that day-to-day reproducibility in the uncertainty budget.

Capacitance gauge calibration, Abbe offset
Abbe offset between the axis of the capacitance gauge and the interferometer axis, coupled with angular motion error of the piezo-electric displacement transducer in the z-direction produces an error in the measured sensitivity factor of the capacitance gauge. The angular motion of the transducer has a linear error of approximately 0,31 μrad/μm, and the Abbe offset is measured to be approximately 3 mm, thus contributing a relative uncertainty of 0,093 % to the height measurement.

Capacitance gauge calibration, cosine error
A cosine error results if the direction of the laser axis is not parallel to the direction of motion of the capacitance gauge. This potential error appears to be limited by the squareness of the connector that fastens the capacitance gauge to the sample platform. An upper limit of 1° is estimated for this error, which leads to a relative uncertainty of 0,0088%.

Capacitance gauge calibration, voltage measurement
Possible nonlinearity in the voltage measurement system for the capacitance gauge contributes a very small uncertainty to the measurement.

Step height measurement, Abbe offset
When a step height measurement is made, any Abbe offset between the capacitance gauge axis and the AFM probe tip leads to an error in the height measurement, when coupled with the angular motion error of the z-stage. This component is similar in form and is estimated to be slightly smaller than the other Abbe uncertainty term described above.

Step height measurement, cosine error
An error in the measured step height could result if the normal direction of the sample surface is not parallel to the direction of motion of the capacitance gauge. This term is

estimated from the apparent slope of the sample surface as the sample is translated over the scan range of 85 μm.

Capacitance gauge nonlinearity

The measured sensitivity of the capacitance gauge varies systematically as the calibration scan length is varied from about 1 μm to about 0,4 μm. This nonlinearity causes uncertainty in the measured step. An estimate of the size of this effect over all measurement scales is made, based on measurements of the change of the measured sensitivity with length.

Algorithm uncertainty

The curvature in the specimen surface should be included in the calculation of step height according to the Nano2 algorithm, but out-of-plane motion due to the instrument should not be included. The C-AFM instrument we used has significant out-of-plane motion, and it is difficult to separate this out-of-plane motion of the instrument from curvature of the specimen. We essentially eliminate the effect of the out-of-plane motion by subtracting a least squares fitted quadratic function from the profiles measured with the C-AFM. However, this procedure may overcorrect the profile because it minimizes the effect of specimen topography in the step height calculation, thus possibly leading to biases in the calculated step height results. We estimate this effect by comparing calculated values of the step height obtained from the Nano2 algorithm with those obtained from an algorithm that essentially eliminates the effect of curvature in the calculated step height results. For these estimates, we used measurements we performed on the Nano2 specimens with the stylus instrument, which has smaller out-of-plane motion than the C-AFM. This procedure slightly overestimates the potential error because the stylus data include both the effect of stylus out-of-plane motion and the sample topography.

Sample stability with respect to cleaning

The Nano2 SH20 step seemed to have a high level of particle contamination when we measured it initially. Then, we crashed the AFM tip on another SH20 specimen and left a number of particles on that surface. Therefore, we decided to clean both samples in order to reduce the number of measurable particles and improve the rms variation in the measured results. We cleaned the samples, then measured them again. The cleaning procedure improved the variation in the results but also seemed to leave the steps with increased step height values on both surfaces. We then decided to repeat the observation again on a third SH20 surface we had. Altogether, we have two sets of stylus data and three sets of C-AFM data comparing the step heights measured before and after cleaning. On the average, the measured step height increased by 0,44 nm. The measured step height therefore seems to be slightly unstable with respect to cleaning. Because we have no knowledge of the state of the Nano2 SH20 sample when it was measured in the laboratories of the other participants, we chose to quote the average value of the results measured for the Nano2 SH20 before and after cleaning and to add a component to the uncertainty budget for this specimen that estimates the potential bias to the measured step height due to either cleaning on the one hand or contamination on the other.

Final Report

Repeatability estimate for the SH20 measurements before cleaning

The data for the Nano2 SH20 before cleaning includes only one topographic image. We estimated the standard deviation for this specimen from image to image by using the standard deviation calculated for the four sets of measurements taken after cleaning then multiplying by a factor that takes into account the observation that the profile-to-profile variation of the measurements taken before cleaning was higher than the profile-to-profile variation of the measurements taken after cleaning. This estimate is calculated to be 0,1294 nm for the SH20 sample.

Those participating in these measurements or in the preparation of the C-AFM tool for these measurements were J. Fu, N.G. Orji, T. Vorburger, T.B. Renegar, R. Köning, and X.Z. Zhao.

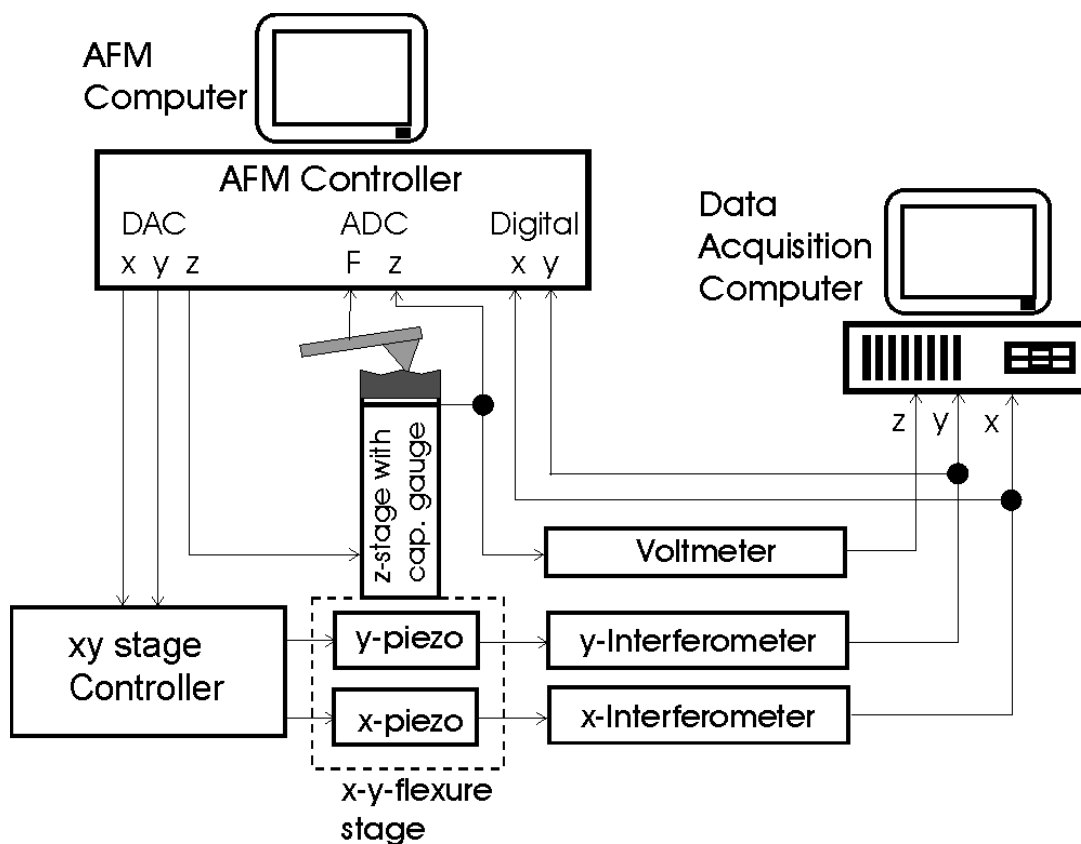Figure 1. Schematic Diagram of the System Design of the C-AFM

References

[1]   R. Dixson, R. Koning, V.W. Tsai, and T.V. Vorburger, Dimensional Metrology with the NIST Calibrated Atomic Force Microscope, *SPIE Proc.* 3677, 20 (1999).

[2]   R. Köning, R.G. Dixson, J. Fu, T.B. Renegar, T.V. Vorburger, V.W. Tsai, and M. Postek, Step Height Metrology for Data Storage Applications, *SPIE Proc.* 3806, 21 (1999).

14 NIST 2 - ST –

Description of the stylus profiling instrument and the measurement methods used

Five Nano2 step height specimens with nominal heights of 7 nm, 20 nm, 70 nm, 300 nm, and 800 nm were measured at NIST with a Talystep stylus instrument interfaced to a personal computer.   We use an interferometrically measured step to calibrate the instrument on each value of magnification employed during a measurement. Profiles of the calibrating step and the step under test are stored in a computer using 16-bit analog to digital conversion. The Nano2 algorithm was used to calculate step height from the measured profiles.

The quoted expanded uncertainty U is equal to the combined standard uncertainty u_c times a coverage factor k (= 2). The combined standard uncertainty u_c is the quadratic sum of the statistical variation of the measurements and five to seven components of uncertainty, related to the instrument and the method of calculation. The statistical variation of the measurements is mainly derived from the uniformity of the specimen under test, but it also includes instrumental random variation during the measurement process. It is calculated as one standard deviation of the mean $(1\sigma_m)$ of the set of values calculated for nine distributed positions along the length of the step. The value at each position is an average of two successive step height values measured there.   Five other components of uncertainty that pertain to the measurement of all five step heights arise from the following sources:

$u(1)$ Height uniformity and surface finish of the step-height master used to calibrate the instrument. This leads to an uncertainty in stylus measurements of the step-height master to obtain the calibration constant of the instrument in the z-direction.

$u(2)$ Variations in the measured calibration constant due to noise in the stylus instrument transducer, surface topography of the reference datum surface for the stylus instrument, sampling and digitizing processes in the controller, and round-off in software computations.

$u(3)$ Biases in the measured step height values due to nonlinearity in the instrument z-transducer.

$u(4)$ Uncertainty in the average height of the step-height master determined from previous interferometric and stylus measurements.

$u(5)$ Uncertainty due to out-of-plane motion of the instrument.   Curvature in the specimen surface should be included in the calculation of step height according to the Nano2 algorithm, but out-of-plane motion due to the instrument should not be included. For the Talystep stylus instrument we used, it is difficult to separate out-of-plane motion of the instrument from curvature of the specimen. This may have led to biases in the calculated step height results.   We estimated this effect by

comparing calculated values of the step height obtained from the Nano2 algorithm with those obtained from an algorithm that essentially eliminates the effect of surface curvature in the calculated step height results. We ascribed the calculated differences to out-of-plane motion of the intrument and assigned uncertainty values to the calculated step heights based on those differences.

In addition to the above uncertainty components, two of the step heights required the consideration of other sources of uncertainty. First, unlike the other step height specimens, the SH70 sample was compared with a step height master having different material, quartz, than the measured step itself, which was coated with chromium. All of the other calibration masters in our laboratory used in these stylus measurements were coated with Cr. The difference in hardness between the master step and the measured step leads to a small bias in the measured step height value. We estimated the size of this effect theoretically and corrected the measured value of the SH70 by a small amount. We also estimated the uncertainty of this correction and included it in the uncertainty budget.

Second, the Nano2 SH20 step seemed to have a high level of particle contamination when we measured it initially. Then, we crashed an AFM tip on another SH20 specimen and left a number of particles on that surface. Therefore, we decided to clean both samples in order to reduce the number of measurable particles and improve the rms variation in the measured results. We cleaned the samples in a solution of Micro 90, then measured them again. The cleaning procedure improved the variation in the results but also seemed to leave the steps with increased step height values on both surfaces. We then decided to repeat the observation again on a third SH20 surface we had. Altogether, we have two sets of stylus data and three sets of C-AFM data comparing the step heights measured before and after cleaning. The root mean square average of the step height increases was 0,44 nm. The measured step height therefore seems to be slightly unstable with respect to cleaning. Because we have no knowledge of the state of the sample when measured in the laboratories of the other participants, we chose to quote the average value of the results measured for the Nano2 SH20 before and after cleaning and to add a component to the uncertainty budget for this specimen that estimates the potential bias to the measured step height due to either cleaning on the one hand or contamination on the other. Nearly all of the components are type A uncertainties, calculated from measured data using statistical methods. The hardness correction for the SH70 step is a type B uncertainty, which was evaluated as a one-standard-deviation estimate from a model that estimates bias in the measured step height values based on the identified uncertainty source. The expressions used for each component depend on the calibration step height H and the measured step height value itself, and on the instrument we used. The six, seven, or eight components are added quadratically to yield the formulas for the combined standard uncertainty for each step.

Those participating in the measurements or in the analysis were T.B. Renegar, T. Vorburger, C.D. Foreman, J.F. Song, and L. Ma.

15 NPL - SPM –

Description of measurement methods and instruments

Measurements were made using the NPL Metrological Atomic Force Microscope (MAFM). This instrument has a commercial atomic force microscope head for servo control of the cantilever, a flexure stage for x/y scanning and interferometric transducers on x, y and z axes for measurement of the relative displacements of tip and sample. 3D images are constructed from the 3 axes interferometer data. Corrections for cyclic non-linearities in the interferometers are applied to the image data before measurement parameters are extracted.

The reference area R1 of each sample was located under the AFM cantilever using an optical microscope. Images were recorded of 16 repeat scan lines across the step at each of 9 locations, evenly distributed along the reference area of the sample. The step height, h, reported for the sample is the average value of the results from the 9 locations

The step height was calculated using the equation

$$ h = \frac{dc\cos(\varphi)}{4nf\cos(\theta)} + L_{abbe}d $$

d is the average vertical distance, in units of optical fringes, between two parallel lines fitted using a least squares algorithm (Cox et al)to the upper and lower regions identified in the technical protocol. The uncertainty in d has been estimated from the quadrature sum of two uncertainty components, the standard error of the mean of the measurements made along the step and an estimate of how repeatably the AFM tip follows the surface.

f is the frequency of the laser used in the z axis interferometer. Its uncertainty is taken from the certificate of calibration.

n is the refractive index of air. Standard atmospheric conditions (air pressure 100000 Pa, temperature 20°C, water vapour pressure 1000 Pa, and CO_2 concentration 400ppm) are assumed and the refractive index calculation from the equations given by Bönsch and Potulski. The uncertainty in n is estimated using these equations and the maximum observed departure from the assumed standard conditions.

L_{abbe} is a correction for the Abbe error due to the angular errors in the AFM head and the non-coincidenece of the z axis measurement axis and the AFM tip. The uncertainty in the value of *L_{abbe}* is calculated from the measured angular errors of the AFM head and an estimate of the maximum distance between the effective measurement axis of the z interferometer and the AFM tip.

Final Report

θ is the angle between the z axis mirror normal and the laser beam.

ϕ is the angle between the normal to the sample surface and the MAFM z-axis.

The sensitivity coefficients appropriate to the equation are, assuming the Abbe term is small compared to h,

References

M G Cox, A B Forbes, P M Harris. Software Support for Metrology Best Practice Guide N0. 4: Discrete Modelling, pp 32-36. National Physical Laboratory, March 200.

G Bönsch, E Potulski. Measurement of the refractive index of air and comparison wuth modified Edlén's formulae. Metrologia, 1998, 35, 133-139.

16 PTB 1 - IM –

Description of the measurement methods and instruments

We used for the measurement a Zeiss interference microscope with automatic fringe evaluation. The instrument is described in full detail in [1]. The light source of the microscope is a thallium lamp (λ=535 nm). The automatic fringe evaluation technique UBSoft was used. The 25x objective with an aperture correction factor k=1,023 was used for the measurement of the 30 µm broad line at reference field R1. The field of view is 160 µm x 160 µm. The fringe pattern was recorded by a 512 x 512 pixel CCD camera with 12 bit amplitude digitalisation. The mean step height is determined at several positions within the reference field R1.

$$\bar{h} = \frac{1}{n_p} \sum_{i=1}^{n_p} h_i \qquad (1.1)$$

Each value h_i is determined from the profile $z_g(x)$ by

$$h_i = \frac{1}{n_u} \sum_{i=1}^{n_u} z_{gui} - \frac{1}{n_l} \sum_{i=1}^{n_l} z_{gli} \qquad (1.2)$$

after alignment using the upper u and the lower ranges of the profile as described in the report. Single data point of the profile z_g where calculated from

$$z_g(x) = z_m - z_{ref} = k * (n+b) * \frac{\lambda}{2} \qquad (1.3)$$

where λ the wavelength of light, k is the aperture correction factor, b is the fringe fraction which is measured by the interference microscope against an internal reference plane. n is the whole number of $\lambda/2$ fringes determined from a measurement by a stylus instrument only providing a rough value for h.

For the calculation of the uncertainty of measurement of the mean step height a model is set up according to the fact that the parameter h is determined from the measured profile $z_g(x)$ (see Appendix A). Here the uncertainty of a the mean height, the single step height, and the single points of the profile is calculated. We take into consideration the wavelength, the aperture correction, reference plane, noise of the instrument, error due to digitalisation and non-linearity of the detector. Further the uncertainty of the evaluation process, due to the focus error, and of the topography is taken into account. Effects due to the phase at the top and at the base of the step, and temperature difference were negligible. For further details see [2, 3].

Uncertainty of measurement

The model for the uncertainty calculation of measurement the mean step height h is structured as in the uncertainty calculation for stylus instruments [2-4]. According to the chain of functions in the device, in a sequence of successive functions P{F[G(z)]}, where z is the row profile data, G the device function, and P the parameter function.

Final Report

1. Uncertainty of the mean height $\overline{h}$

$$\overline{h} = \frac{1}{n_s} \sum_{i=1}^{n_s} h_i + \delta h_{Topo} + \delta h_{Focus} + \delta h_{\Delta\varphi_{u,l}} + \delta h_{\Delta T}$$

where h_i is single height value, measured n_s times

δh_{Topo} - the standard deviation of the height,

δh_{Focus} - the influence due to the focus on the area used for step height determination,

$\delta h_{\Delta\varphi_{u,l}}$ - the influence due to different phase at top of the step and bottom, and

$\delta h_{\Delta T}$ - influence due to temperature difference.

$$u^2(\overline{h}) = (\frac{\partial \overline{h}}{\partial h_i})^2 u^2(h_i) + u^2(\delta h_{Topo}) + u^2(\delta h_{Focus}) + u^2(\delta h_{\Delta\varphi_{u,l}}) + u^2(\delta h_{\Delta T})$$

$$u^2(\overline{h}) = \sum_{i=1}^{n_s} \frac{1}{n_s^2} u^2(h_i) + u^2(\delta h_{Topo}) + u^2(\delta h_{Focus}) + u^2(\delta h_{\Delta\varphi_{u,l}}) + u^2(\delta h_{\Delta T})$$

With $u^2(h_i) = u^2(h)$

$$u^2(\overline{h}) = \frac{1}{n_s} u^2(h) + u^2(\delta h_{Topo}) + u^2(\delta h_{Focus}) + u^2(\delta h_{\Delta\varphi_{u,l}}) + u^2(\delta h_{\Delta T})$$

$$u^2(\overline{h}) = \hat{N}_s u^2(h) + u^2(\delta h_{Topo}) + u^2(\delta h_{Focus}) + u^2(\delta h_{\Delta\varphi_{u,l}}) + u^2(\delta h_{\Delta T})$$

The operator $\hat{N}_s$ only interacts on random components.

2. For the next step we investigate the single height value h.

$$h = \overline{z}_{gu} - \overline{z}_{gl} + \delta h_{align}$$

where

$\overline{z}_{gu,l}$ - are the average value at upper and lower plane after alignment of the profile, respectively, and

δh_{align} - is the error due to alignment of the profile.

Final Report

$$h = \frac{1}{n_u} \cdot \sum_{i=1}^{n_u} z_{gui} - \frac{1}{n_l} \cdot \sum_{i=1}^{n_l} z_{gli} + \delta h_{align}.$$

$\overline{z}_{gu,li}$ - are the single points of the profile at positions used for height determination.

The uncertainty of h is calculated as

$$u^2(h) = \sum_{i=1}^{n_u} \left(\frac{\partial h}{\partial z_{gui}} \right)^2 \cdot u^2\left(z_{gui} \right) + \sum_{i=1}^{n_l} \left(\frac{\partial h}{\partial z_{gli}} \right)^2 \cdot u^2\left(z_{gli} \right) + u^2(\delta h_{align})$$

Assuming $\dfrac{\partial h}{\partial z_{gui}} = \dfrac{1}{n_u}$ and $\dfrac{\partial h}{\partial z_{gli}} = \dfrac{1}{n_l}$ for i=1 to n_u or n_l respectively with $u(z_{gui}) = u(z_{gli}) = u(z_g)$ gives

$$u^2(h) = \left(\frac{1}{n_u} + \frac{1}{n_l} \right) u^2\left(z_g \right) + u^2(\delta h_{align})$$

$$u^2(h) = \hat{N}_{u,l} u^2\left(z_g \right) + u^2(\delta h_{align})$$

with

$$\hat{N}_{u,l} u^2(z_g) = \left(\frac{1}{n_u} + \frac{1}{n_l} \right) u^2(z_g),$$

where the $\hat{N}_{u,l}$ only acts on random uncertainty contributions.

3. In the next step we investigate the single profile value.

For the single value z_g the model is:

$z_g = z_m - z_{ref}$

This is the difference of the two topographies of the sample and reference mirror measured. For details see R. Krüger-Sehm [3,4]. The result is:

$$z_g = n \cdot k \cdot \lambda + h_m + \delta \overline{z}_{ref} \sqrt{1 + \frac{1}{q}} \cdot \left(\delta z_{noise} + \delta z_{noise} \right) + \sqrt{2} \cdot \delta z_{nl}$$

where:

n   - integer number of fringes

k - aperture correction

λ - wavelength of light

h_m - height of measured step (only fraction of fringe)

δz_{ref} - reference mirror

q   - number of averages to determine the ref. mirror

δz_{noise} - noise of the instrument

δz_{dig} - digitalisation error

$\delta z_n l$ - non-linearity

The uncertainty of z_g is

$$u^2(z_g) = h^2 \cdot u_{rel}^2(\lambda) + h^2 \cdot u_{rel}^2(k) + u^2(\delta \overline{z}_{ref}) + (1 + \frac{1}{q}) \cdot \left(u^2(\delta z_{noise}) + u^2(\delta z_{noise}) \right) + 2 \cdot u^2(\delta z_{nl})$$

4. Taking all contributions into account we get for the uncertainty of $\overline{h}$:

$$u^2(\overline{h}) = h^2 \cdot u_{rel}^2(\lambda) + h^2 \cdot u_{rel}^2(k) + u^2(\delta \overline{z}_{ref})$$

$$+ \hat{N}_s \hat{N}_{u,l} (1 + \frac{1}{q}) \cdot \left(u^2(\delta z_{noise}) + u^2(\delta z_{dig}) \right) + 2 \cdot N_s \hat{N}_{u,l} \hat{u}^2(\delta z_{nl})$$

$$+ \hat{N}_s u^2(\delta h_{align}) + u^2(\delta h_{align}) + u^2(\delta h_{\Delta T}) + u^2(\delta h_{Focus}) + u^2(\delta h_{\Delta \varphi u,l}) + u^2(\delta h_{Topo})$$

References:

[1] U. Brand and W. Hillmann, Calibration of step height standards for nanometrology using interference microscopy and stylus profilometry, Prec. Eng. 17 (1995) 22-33

[2] R. Krüger-Sehm, M. Krystek, Proceedings DIN-Session "GPS 99", 5-6- May 1999, p. 3-1 – 3-17

[3] R. Krüger-Sehm and M. Krystek, Uncertainty analysis of roughness measurement, Proc. of X. Int. Colloquium on Surfaces and Tutorials, Chemnitz, Jan. 31st – Feb. 1st, 2000, Additional Papers

[4] R. Krüger-Sehm, J. A. Luna Perez, Int. Journ. of Machine Tools & Manufacture, 41 (2001) p. 2123 – 2137

17 PTB 2 - SPM –

Description of the measurement methods and instruments

The high resolution scanning force microscope (SFM) used is a modified instrument based on the VERITEKT manufactured by Carl Zeiss Jena. One can compare the Veritekt to a miniaturised three-coordinate measuring machine. The scanner block realises the motions in the three axes, x, y, and z. The measuring range is (x, y, z)=(70, 15, 15) μm and the resolution (x, y, z)=(1,25; 0,25; 0,25) nm. This SFM is of the scanning sample type and the cantilever with optical auto-focus sensor served as the zero indicator in the z-direction. The signal of the auto-focus sensor is used for the feedback controller of the z-position of the sample. The z-values are used to determine the surface topography of the sample to be measured.

The instrument has three piezos with integrated capacitive transducers for positioning control during scanning. Those capacitive transducer are calibrated by using three integrated laser interferometers assigned to the axes of motion x, y, and z of the sample holder. The calibration is performed parallel to the Abbe directions of the mounted sample. The interferometers deliver a grid of defined calibration points at the distance of half the wavelength of the used He/Ne laser radiation between neighbouring points. About 6000 calibration points are used in the measuring range. The resolution of the laser interferometers is 0,1nm, their expanded uncertainty of measurement is ≤ 1 nm. The calibration procedure is carried out before and after high-quality measurements, thus giving information about the stability of the calibration. This ensures traceability of the measurement to the unit of length. Deviation of the scanner from ideal motion, due to cross-talk, etc., have been measured and minimised by correction tables in the control software. This development was realised in several steps in co-operation with the Ilmenau Technical University (see Fig. 1 and 2). [1,2,3]
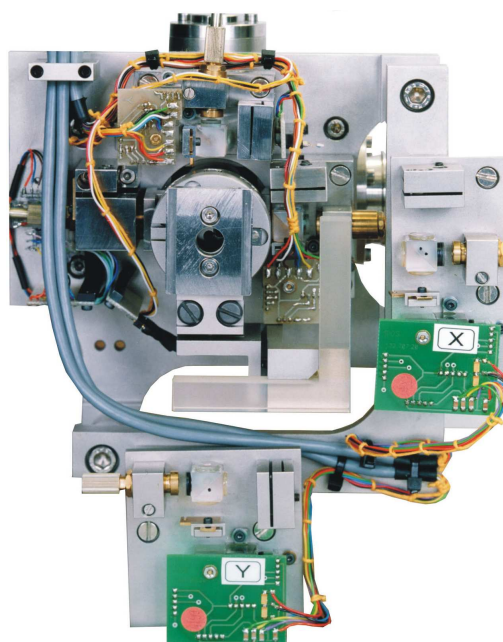

Fig. 1. View of the scanner block with sample holder. The L-shaped mirror serves for the interferometric measurement of motions in the x- and y-directions.
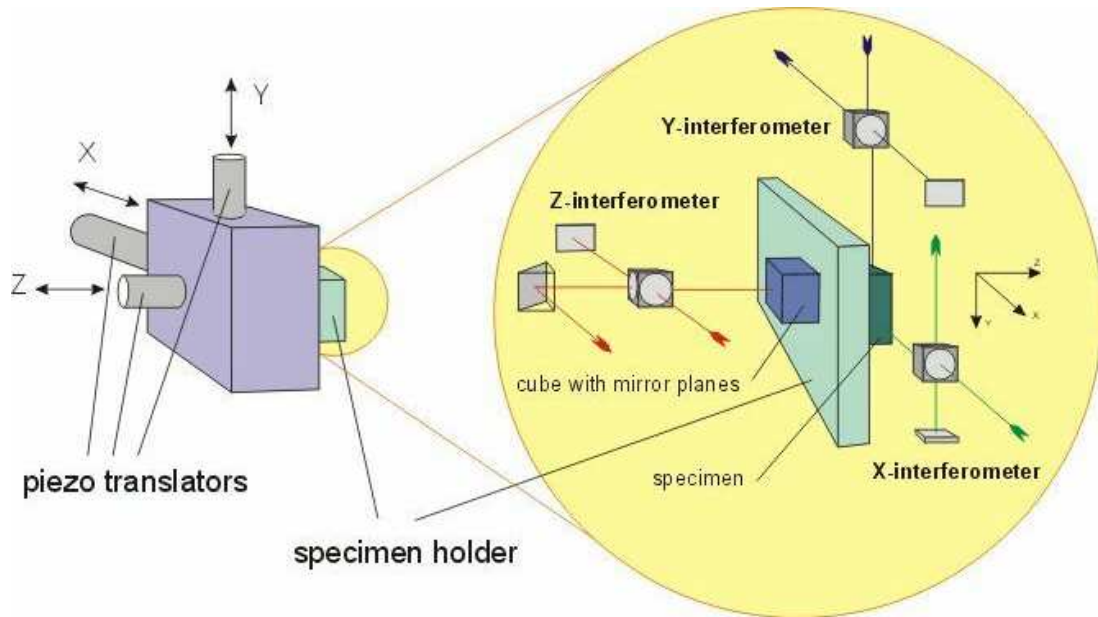
Fig. 2. Optical arrangement of the laser interferometers in the SFM avoiding the Abbe error
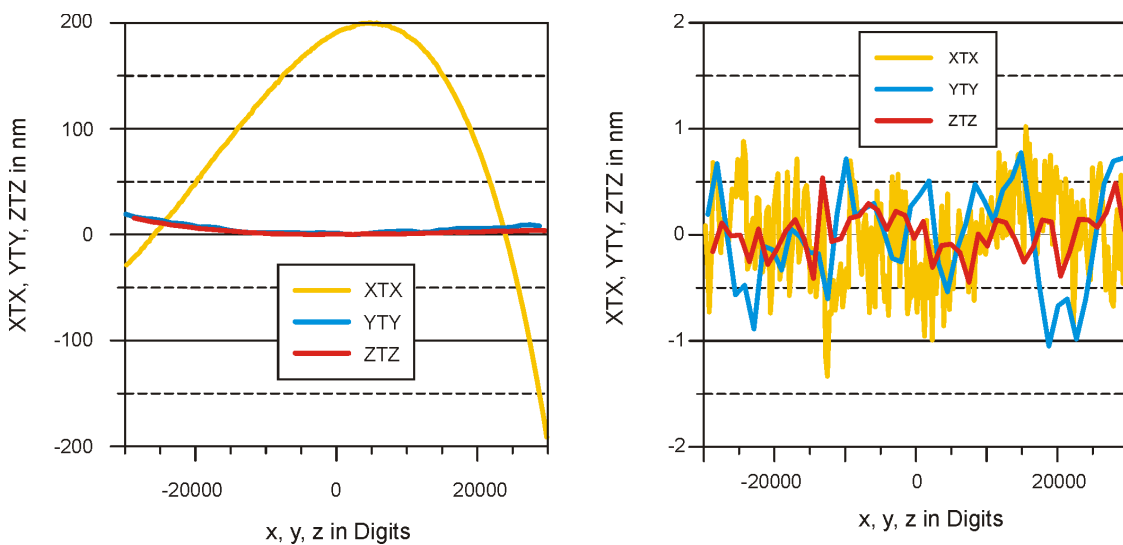
Fig. 3. Errors of the scanner movement in the directions x, y, and z remaining before (left) and after (right) the compensation of the non-linearity of the scales, the cross-talk and the non-orthogonality between the axes on the basis of laser interferometer measurement

The calibration procedure is fully automated and can be carried out within 35 minutes. Fig. 3 on the left side depicts the errors of the scanner movement in the directions x, y, z (position errors each XTX, YTY, ZTZ) based on the original capacitive measuring system. The right side then shows the errors of the scanner movement after the compensation of the non-linearity of the scales, the cross-talk and the non-orthogonality between the movement axes on the basis of laser interferometer measurements.

The measurement strategy and evaluation

The step height h was evaluated at five different locations P1 to P5 distributed equally over the area R1 (see Figure 4) with the same tip. On each location 10 to 15 images were recorded with the edge parallel to the y-axis. The size of each scan was 65 µm x 3,5 µm using 600 points and up to 32 lines. The average step height h_i for each location was calculated from the average step height h_{ij} of all lines of the j-image at position i choosing a line by line fit of first order. The software SPIP 2.21 [4] used allows to calculate the step height as described in the ISO 5436. The average step height $<h>$, that is the measurand, was calculated as the average step height from the five values h_1 to h_5. This procedure takes into account the variation of the step height over the measurement area.
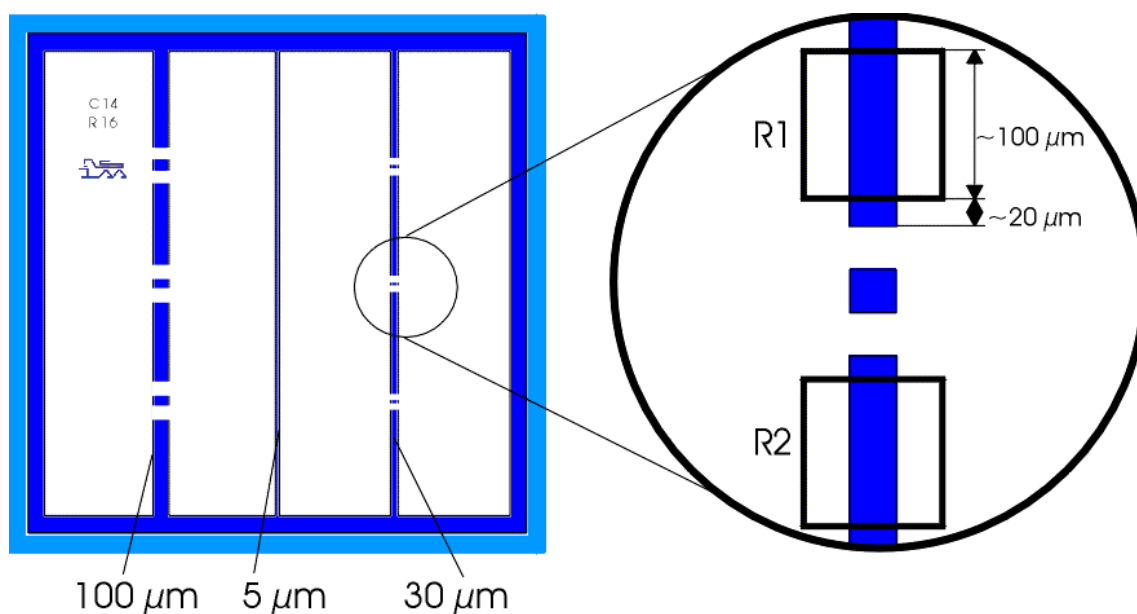
Fig. 4. Picture showing the sample design (left), the location and the dimensions of measurement area R1 (right)

The uncertainty

In the following the contributions are listed which were taken into account for the budget of measuring uncertainty.

1. Uncertainty of laser wavelength λ_{vac}

2. Uncertainty of refractive index $n(p,T,h,..)$ during calibration

3. Alignment of interferometric z-axis to the axis of movement (cosinus error) $\delta z_{cos(\alpha)}$

4. Interferometric dead path error $\delta h_{dp} = \Delta n_* s / n_2$, with $n_2 = n_1 + \Delta n$

5. Short term stability of calibration $\delta C_z(\lambda_{vac}, n)$

6. Non-linearity of the calibration of the z-axis $\delta h_{ztz} = C_z * \delta z_{ztz}$

7. Uncertainty due to cross-talk in z-direction caused by movement in x direction and y-direction (out of z-plane movement) $\delta h_{xtz} = C_z * \delta z_{xtz}$ and $\delta h_{ytz} = C_z * \delta z_{ytz}$, respectively.

8. Uncertainty due to the tilt of the sample to the scanning plane combined with the drift in the y-direction $\delta h_{\text{y-drift}}$.

9. Uncertainty of the z-position due to finite step response time (step up and step down) $\delta h_{\text{z\_response}} = C_z * \delta z_{\text{z-response}}$

10. Uncertainty due to non-coincidence of the z-measurement axis and the zero point detector (cantilever tip) $\delta h_{\text{0-Abbe}}$

11. Uncertainty due to drift of the zero point detector in z-direction $\delta h_{\text{0-drift}}$

12. Uncertainty due to wear of the probe δh_{wear}

13. Uncertainty due to different elastic/plastic deformation at different locations (extrapolation to F $\rightarrow$ 0) $\delta h_{\text{elastic}}$

14. Uncertainty due to other interaction forces during scanning (van der Waals, lateral forces) $\delta h_{\text{vdW,xy}}$

15. Uncertainty of the determination of the step height from the profile (roughness of the sample) $\delta h_{\text{align}} = C_z * \delta z_{\text{align}}$

16. Noise and digital resolution of the instrument z-axis z_{noise}

17. Uncertainty due to the non-uniformity of the sample δh_{topo}

18. Uncertainty due to a temperture difference of the sample to 20 °C δh_{therm} ($T_s \neq 20$ °C)

$$< h > = \frac{1}{n_p} \sum_{i=1}^{n_p} h_i + \delta h_{wear} + \delta h_{elastic} + \delta h_{vdW,xy} + \delta h_{topo} + \delta h_{therm} \qquad (1.1)$$

$$h_i = C_z(\lambda, n) * \Delta z + \delta h_{dp} + \delta h_{z-response} + \delta h_{y-drift} + \delta h_{0-Abbe} + \delta h_{0-drift} \quad (1.2)$$

$$\Delta z = < z_{u,l} > = \overline{z}_u - \overline{z}_l + \delta z_{align} = \frac{1}{n_u} \sum_{i=1}^{n_{u,l}} z_{ui} - \frac{1}{n_l} \sum_{i=1}^{n_l} z_{li} + \delta z_{align} \qquad (1.3)$$

$$z_i = z_m - z_{ref} = z_m + \delta z_{noise} + \delta z_{ztz} + \delta z_{xtz} \qquad (1.4)$$

The uncertainty is

$$u^2(<h>) = \sum_{i=1}^{n_p} u^2(h_i) + u^2(\delta h_{wear}) + u^2(\delta h_{elastic}) + u^2(\delta h_{vdW,xy}) + u^2(\delta h_{topo}) + u^2(\delta h_{therm})$$
$$= \hat{N}_p u^2(h_i) + u^2(\delta h_{wear}) + u^2(\delta h_{elastic}) + u^2(\delta h_{vdW,xy}) + u^2(\delta h_{topo}) + u^2(\delta h_{therm}) \qquad (2.1)$$

where $\hat{N}p = \dfrac{1}{n_p}$ only acts on random contributions of $u(h_i)$.

$$u^2(h_i) = h_i^2 \frac{u^2(\lambda)}{\lambda^2} + h_i^2 \frac{u^2(n)}{n^2} + h_i^2 \frac{u^2(\cos \alpha_z)}{\cos \alpha_z^2} + h_i^2 u^2(\delta C_{z,Drift}) + C_z^2 * u^2(\Delta z) + u^2(\delta h_{dp})$$
$$+ u^2(\delta h_{z-response}) + u^2(\delta h_{y-drift}) + u^2(\delta h_{0-Abbe}) + u^2(\delta h_{0-drift}) \qquad (2.2)$$

Final Report

$$u^2(\Delta z) = u^2(<z>) = n_u \left(\frac{1}{n_u}\right)^2 u^2(z_{ui}) + n_l \left(\frac{1}{n_l}\right)^2 u^2(z_{li}) + u^2(\delta z_{align})$$

Using $z_{ui} = z_{li} = z_i$ gives

$$u^2(<z>) = \left(\frac{1}{n_u} + \frac{1}{n_l}\right) u^2(z_i) + u^2(\delta z_{align}) = \hat{N}_{ul} u^2(z_i) + u^2(\delta z_{align}) \qquad (2.3)$$

where $\hat{N}_{ul} = \left(\dfrac{1}{n_u} + \dfrac{1}{n_l}\right)$ only acts on random contributions.

$$u^2(z_i) = u^2(\delta z_{noise}) + u^2(\delta z_{ztz}) + u^2(\delta z_{xtz}) \qquad (2.4)$$

A coarse estimation of the above contributions (see table 1):

1. Uncertainty of laser wavelength λ_{vac} $u(\lambda_{vac})/\lambda_{vac} = 10^{-7}$. The maximum step height is 800 nm. This gives $(800nm*10^{-7}) \leq 8*10^{-5}$ nm. The error of wavelength can be neglected.

2. Uncertainty of refractive index $n(p,T,h,..)$ during calibration $u(n)/n=10^{-6}$. This gives $800nm*10^{-6} \leq 8*10^{-4}$ nm.

3. Alignment of interferometric z-axis to the axis of movement (cosinus error) $\delta z_{cos(\alpha)}$.

4. Interferometric dead path error $\delta h_{dp} = \Delta n_* d/n_2$, with $n_2 = n_1 + \Delta n$. The environment parameters are measured during calibration. The calculated refractive index is used to correct the wavelength. From this the change Δn is less than 10^{-7}, $u(n)$, and $u(\Delta n)$ less than 10^{-8}, the dead path of the interferometer d is zero, and the uncertainty $u(d)=1mm$.

5. Stability of the calibration. This includes the stability of the electronic and the mechanics of the scanning part. Any drift of the electronic and mechanic pretends a height change. We assume this value from the difference of the calibration factor $\delta C_z(\lambda_{vac},n)$ (before and after measurement). This change is less than $1*10^{-4}$.

6. Non-linearity of the calibration of the z-axis δz_{ztz}. The residual non-linear error in z-direction ztz is smaller than $2*10^{-4}*h+0,5nm$. For 800 nm this results in 0,65 nm.

7. Uncertainty of cross-talk in z-direction due to movement in x direction (out of z-plane movement) δh_{xtz}. The residual cross-talk error in z direction when x axes moving xtz is smaller than 1,0nm. Since only single lines are evaluated the cross-talk of the y-axis which is kept fix during a profile scan can be neglected.

8. Due to the tilt of the sample a drift in the y-direction causes an uncertainty in the height which could not be corrected by a plane fit. This error is given by $\delta h_{y-drift} = \delta y_{drift}*\tan(\alpha_y)$. α_y is the angle of the sample to an ideal plane during the scan.

9. Uncertainty of the z-position due to finite step response time $\delta h_{z-response}$. Could be neglected due to the feedback parameters, the speed chosen, and the evaluation method by using non-edge data.

10. Uncertainty due to non-coincidence of the z axis measurement axis and the zero point detector tip δh_{0-Abbe}. The deviation δh_{0-Abbe} between calibrated z-axis and zero point is assumed to be $\delta h_{0-Abbe} < 0,5mm$.

11. Uncertainty due to drift of the zero point detector in z-direction $\delta h_{0-drift}$. Drift of zero sensor during the x-scan in the z-direction.

12. Uncertainty due to wear of the probe δh_{wear}. The pictures did not show any degradation of the tip. We assume a tip wear of 10 nm over the 32 lines x 15 repeated images x the five position. Wear for one line is 10 nm/32/15/5 < 0,01 nm.

13. Uncertainty due to the force (extrapolation to F $\rightarrow$ 0) $\delta h_{elastic}$. The tip and the sample surface are deformed during the contact scan [5]. The difference of the deformation δ_0 of tip and sample at base (silicium substrate) and at top (SiO_2 line) is different by 55pm for a tip radi of R=50 nm and a force of 10^{-9}N.

14. Uncertainty due to other interaction forces during scanning (adhesion, van der Waals forces, lateral) $\delta h_{vsW,xy}$. Adhesive layers are not known. We assume no influence of a different deformation of the tip at bottom and on the top of a line. The roughness at the bottom an d the top of a line is determined by the chromium coating of the whole sample. Therefore equal friction forces are acting on the tip during the scan (except for the edges of the line).

15. Uncertainty of the determination of the step height from the profile (roughness of the sample) δz_{align}. The roughness value Pt determines the uncertainty of a single line fit. The distribution is rectangular. This is given by $1/\sqrt{3}*(Pt/2)$. In this case we observe the height from a large number of lines at each point. Therefore Pt is replaced by Sq.

16. The random contribution (noise) to u(Δz) is estimated from the repeatability $\sigma(h_{ij})$of the determination of the step height at the same place.

17. Uncertainty due to the non-uniformity of the sample δh_{topo} is estimated from the standard deviation between the five points σ_{std},

18. Uncertainty due to the thermal expansion at measurement temperature δh_{therm}. For the maximum step height standard 800 nm, a maximum temperature difference of 1 K and the thermal expansion coefficient of $2,6*10^{-6}$/K of silicon gives a maximum uncertainty contribution of $2*10^{-3}$nm. This contribution can be neglected.

References

[1]   M. Bienias, S. Gao, K. Hasche, R. Seemann, K. Thiele: A metrological scanning force microscope used for coating thickness and other topographical measurements, Applied Physics A66, S837-S842 (1998)

[2]   K. Thiele, K. Hasche, K. Herrmann, R. Seemann: Determination of the geometry of micro hardness indenters using a calibrated scanning force microscope, Proc. 3rd Seminar on Quantitative Microscopy, Lyngby, Denmark, PTB-F-34, Braunschweig, December 1998, ISBN 3-89701-280-4, 115 – 122

[3]   K. Herrmann, K. Hasche, F. Pohlenz, R. Seemann: On some metrological applications of Scanning Force Microscopy, Poster on Workshop „Scanning Probe Microscopy in Nanotechnology" at the Technical University Wroclaw, 10./11.7.01

[4]   The Scanning Probe Image Processor SPIP™, User's and Reference Guide. Image Metrology

[5]   M. A. Lantz et al., Rhy. Rev. B, 55 (1997) 10776

Table 1: Listed contributions of uncertainty components (h=800nm)

No	Description	X	Value / Estimation	D	u(X)	ci(h)	ui(h) /nm
1	Wavelength	λ_{vac}	632,8 nm	N	1,00E-07	777,8	0,0001
2	*Refr. Index*	*n*	1,00027	N	1,00E-06	777,8	0,0008
3	Cosinus(l,z)	$\cos(\alpha_z)$	$\alpha_z \leq 1°$	R	4,33E-05	777,8	0,0337
4	Dead path error	δh_{dp}	d_{dp}=0 mm, u(d_{dp})=1mm $\delta n=10^{-7}$, u(δn)=10^{-8}	N	0,1	1	0,1000
5	z-Scale	$\delta C_z(\lambda,n)$	$\leq 2*10^{-4}$	R	5,77E-05	777,8	0,0449
6	Non linearity	δh_{ztz}	$\leq 2*10\text{-}4*h+0,5$ nm	R	0,1892	1	0,1892
7	Cross talk x	δh_{xtz}	$\leq 1,0$ nm	R	0,2887	1	0,2887
8	y-drift	$\delta h_{y\text{-}drift}$	$\tan(\alpha_{yz})$<100nm/10µm, Δydrift<100nm/h 32 lines, 20 Min.,600 points/line 20 points at transition	N	3,47E-05	1	0,0000
9	Feedback	$\delta h_{z\text{-}response}$	$\leq 0,01\%$	R	2,89E-05	777,8	0,0225
10	Zero point alignment	$\delta h_{0\text{-}Abbe}$	$\delta h_{0\text{-}Abbe}$< 0,5 mm, zrx<0,1",zry<0,1"	N	0,4848	1	0,4848
11	Zero point drift	$\delta h_{0\text{-}drift}$	$\delta h_{0\text{-}drift} \leq_3 0$ nm/h, Δt=20min,32 lines	R	0,0902	1	0,0902
12	Tip wear	δh_{wear}	$\delta h_{wear} \leq 10$nm, 32 lines/ 15 images/5 positions	R	0,0012	1	0,0012
13	Deformation of tip and surface at base and top of the	$\delta h_{elastic}$	$\leq 0,055$ nm	R	0,0159	1	0,0159
14	Torsion of tip	δh_{tip}	$\leq 0,01$ nm @ 5 nm/5µm	R	0,0014	1	0,0014
15	Alignment error	$C * \delta z_{align}$	$1/\sqrt{3} * (Ra/2)$	R	0,8372	1	0,8372
16	Reproducibility	δh_{rep}	$1/\sqrt{Ns} * \delta hrep$	N	0,1229	1	0,1229
17	Topography	δh_{topo}	$1/\sqrt{Np} * \delta htopo$	N	0,5443	1	0,5443
18	Temperature	δh_{therm}	$1/\sqrt{3} * (2,6*10^{-6}/K*1K)$	N	1,50E-06	777,8	0,0012
						u(h)=	1,18
						U(k=2)=	2,4

18 PTB 3 - ST –

Description of the measurement methods and instruments

A commercial Nanostep (Taylor-Hobson) stylus instrument was used for data collection. The properties of this instrument have been described in [1] and ref. therein. For data evaluation and storage, a home made system was used. All measurements were performed with a stylus of 2 µm radius, a force of 25 µN, and a low traverse speed of 5 µm/s. The lowest traverse speed was used to achieve optimum profile resolution of 0,1 µm over the trace length of 100 µm centred at line. Five traces were made within the reference field R1. The calibration of the vertical axis of the Nanostep were carried out for the different ranges using the SMU standards [2] calibrated by interference microscope. The profiles obtained are analysed using the software UBSoft.

Measurement results and uncertainty evaluation following the GUM take into consideration the uncertainty of the standard, the reference plane, noise of the instrument, error due to digitalisation and non-linearity, and the uncertainty of the evaluation process. For further details see [3].

[1] U. Brand and W. Hillmann, Calibration of step height standards for nanometrology using interference microscopy and stylus profilometry, Prec. Eng. 17 (1995) 22-33

[2] H. Haitjema, International comparison od depth setting standards, Metrologia, 34 (1997) 161-1267

[3] R. Krüger-Sehm and M. Krystek, Uncertainty analysis on roughness measurement, Proc. of X. Int. Coll. on Surfaces (Additional Papers), Chemnitz 2000

19 VNIIM 1 - LHI –

Description of the measurement methods and instruments

Set-up for step height measurement is laser heterodyne interferometer with a single-frequency He-Ne laser and acousto-optical modulators.

There is the optical scheme of the interferometer:

Modulators operate in a normal-incidence mode with symmetric diffraction spectrum. Measurement and reference beams are resolved on the standard's surface, with the spots diameter approximately 12 μm, and 100 μm distance between the spots. Two alternative interference signals (measuring and reference) are registered by photomultipliers and it's phase difference is measured by digital phasemeter. The step height is determined from the phase difference bounds which occur in lateral translation of the standard.

Long-term stability of the phase difference was less then 0,1°. Investigation of the interferometer transfer function linearity reveal periodic deviation of the measured phase difference, which may be reduced to 0,2° by thorough alignment of the set-up.

Phasemeter uncertainty is 0,1°.

The standard is slightly tilted in order to prevent the light, reflected from the standard, from returning directly to the laser. It results in cosine correction factor in the step height expression.

Another correction factor deals with the beam's focusing at the surface of the sample. The phase of the wave-front traversing the axes of the gaussian beam at a distance z from the waist is defined by expression [H. Kogelnik, T. Li. Laser Beams and Resonators. Proceedings of the IEEE, V54, No. 10, 1966, p. 1312-1329]

$$\phi_{gauss} = -kz + arctg \frac{\lambda \cdot z}{\pi \cdot \omega_0^2},$$

were $k = \frac{2\pi}{\lambda}$, $2\omega_0$ - diameter of the waist.

Assigning an "effective" wave-length in Gaussian beam as $\lambda_{eff} = -\dfrac{2\pi}{\partial\phi_{gauss} / \partial z}$,

we can find the correction factor for the wave length at the vicinity of the waist as $(1+(\lambda/\pi\omega_0)^2/2)$.

Resulting expression for the step height is:

   h=$((\Delta\varphi + n \cdot 360)/360) \cdot \lambda /2 \cdot (1+(\lambda /\pi\omega_0)^2/2) \cdot (1/\cos \alpha)$,

were $\Delta\varphi$ is the measured phasechange (°) ,

n - integer,

λ - laser wavelength,

ω_0 - radius of the laser beam spot on the surface of the standard,

α - angle of incidence of the beam onto the standard's surface.

20 VNIIM 2 - µI –

Description of the measurement methods and instruments

The height of the step height standards was determined by aid of the laser Michelson microinterferometer which was illuminated by the light of the Ar or He-Ne lasers. The sample (standard) was placed in the first arm of the interferometer and was oriented perpendicular to the laser beam. The mirror was placed in the second arm. All measurements were carried out with the mirror tilted slightly with respect to the optical axis, thus were produced several interference fringes in field of view. The tilt direction was such that the fringes crossed of the rectangular step. The step interference images were fixed with two objectives at the microscope focal plane. The spatial filtration allowed a selection of pair of the beams. After the microscope the phase interference image of the step was recorded by a 736x572 pixel CCD camera then was emitted to a computer. The phase difference between lower and upper flatness of step (φ +N) measured for the step height (h) determination according to the following equation:

$$h=(\varphi +N)\frac{\lambda}{2},$$

with φ -fractional part of interference order, N- whole number and λ -the laser wavelength.

The computer analysed the phase of the light for each pixel and calculated the average step height and type A standard uncertainty. On each standard measurement cycles more suitable from the five different wavelengths were performed. The laser vacuum wavelengths and the wavelength uncertainties given in "Handbook of lasers with selected date on optical technology" (Edited by R.J.Pressiey. Chemical Rubber Co, Cleveland, 1971). Pressure, temperature and humidity were monitored to calculate the refraction index of the air by the Edlen formula .

The most important type B standard uncertainty sources were the defocus effect and interference evaluation. A test was carried out by measuring the step height standard many times with different setting of the microscope focal plane .The sample tilt uncertainty was estimated at θ_α=4*10^{-6} .The measurements were made on the reference temperature of $20^o C$ with standard uncertainty u(t)=0,5^o C.

Final Report

Appendix B: Time schedule (detailed)

Lab.	Country	Originally schedule	Confirmation of reception	Comment	Results received
PTB	Germany	1.9.2000	./.	IM and TS, *)	1.9.2000
IMGC	Italy	1.10.2000	22.9.2000	no damage cantilever on SH800 cleaning at PTB	2.4.2002
NMi-VSL	Netherlands	1.11.2000	15.11.2000	small amount of dust particles outside the measurement area. This is of no consequence.	9.1.2001
CEM	Spain	1.12.2000	12.12.2000	no damage	7.3.2001
DFM	Denmark	15.1.2001	No conform.	./.	4.2.2002
PTB	2nd circle			by passed to METAS	
METAS	Switzerland	1.3.2001	22.2.2001	All standards have considerable amount of impurities present at the surface.	8.4.2001
NIM	China	1.7.2001	4.4.2001	no damage	3.4.2002
CMS	Taiwan	1.5.2001	18.5.2001	no damage	27.11.2001
NMIJ	Japan	1.6.2001	8.6.2001	no damage cantilever on SH300 cleaned at NMIJ	28.9.2001
KRISS	Korea	1.8.2001	20.7.2001	Scratch on SH300 between the ref. Fields R1 and R2	6.5.2002

Final Report

PTB	3rd circle	1.9.2001	5.9.2001	IM and TS	
NPL	United Kingdom	1.10.2001	11.10.2001	Scratch on SH300, Mark on SH800 Tip crash on SH300	20.2.2002
PTB			31.10.2001 11.11.2001	Cleaning SH300, back to NPL	
PTB			16.11.2001	by passed to GUM	
GUM	Poland	1.11.2001	7.12.2001	No damage	25.2.2002
				The general conditions of the step height standards and the reference area (R1 and R2) is good. However on the remaining flats of standards, in particular SH020, there are very small spots. Additionally on SH300 between the areas R1 and R2 there is a scratch(?). But they are not situated on the flats R1 and R2.	
PTB			14.1.2002	23.1.02 by passed to VNIIM	
VNIIM	Russia	1.12.2002	18.2.2002	After visual and optical inspection no damage has been observed.	29.4.2002
PTB			12.4.2002	12.4.02 by passed to NIST	
NIST	USA	1.4.2001	18.4.2002	Detailed description of the samples, problems with SH70, SH20, SH7 Cleaning of SH20 at NIST	
PTB			5.6.2002	Cleaning SH007 and back to NIST	
NIST	USA		14.6.2002	SH007 at NIST	5.9.2002
PTB		15.1.2002	9.7.2002	All samples back at PTB. IM, TS, SPM*)	3.9.2002

*) At the failure of the first set of standards, the metrology SPM of the PTB was moving from Berlin to Braunschweig and was not available for measurements. Due to some time delays in Sept. 2001, it was not possible to measure before July 2002.

Final Report